

**Mohammad Aljaradin**

Division of Water Resources Engineering  
Department of Building and Environmental  
Technology  
Lund Institute of Technology, Lund University

Courses during Doctoral Study.

**-Hydrodynamics of lakes and reservoirs (October 2011)**

# Hydrodynamics of Lakes and Reservoirs

General processes: focus on  
stratification

ERASMUS LECTURES PREPARED FOR  
LUND UNIVERSITY

**Assoc.Prof.Dr.ŞEBNEM ELÇİ**

IZMIR INSTITUTE OF TECHNOLOGY

CIVIL ENGINEERING DEPT.

# Who am I ?

- I am currently working as **Associate Professor** at Izmir Institute of Technology, Civil Engineering Department
- I have graduated as Civil Engineer in 1995 from METU.
- I have graduated from Georgia Institute of Technology with an emphasis on Environmental Fluid Mechanics and Water Resources
- Since my enrollment as faculty in Civil Engineering Department of Izmir Institute of Technology in 2004, I coordinated two scientific projects; one funded by national science foundation (*TUBITAK Project No:104Y323*) and the other by the European Commission (*Marie Curie International Re-Integration Grant No: 28292*) and participated as investigator in four others (*TUBITAK Projects No: 104M301; 106M274; 110M240*) of which were related to hydraulics, sediment transport and water resources management issues.
- I have written over 30 papers, including 9 journal articles indexed by Web of science (SCI).
- I have served as ***Vice Dean of the Engineering Faculty, Vice Chair and Departmental Chair of Civil Engineering*** since my enrollment.
- I am recipient of the ***Marie Curie International Reintegration Grant*** given by the European Commission (2005), and was awarded ***Rising Star Trophy*** for Research by Clemson University (2002).
- I am married and have a 6 yr old daughter.

# Izmir Institute of Technology

- A state institution established in 1992; IYTE places emphasis on research and graduate and undergraduate education in fields relevant to science and technology and on interdisciplinary studies.
- The language of instruction is English.
- At our institute educational and research activities are carried out in 10 undergraduate, 25 master's and 12 doctorate programs with a total of 2,200 students, 1600 of which are here for their undergraduate education.



# Izmir Institute of Technology

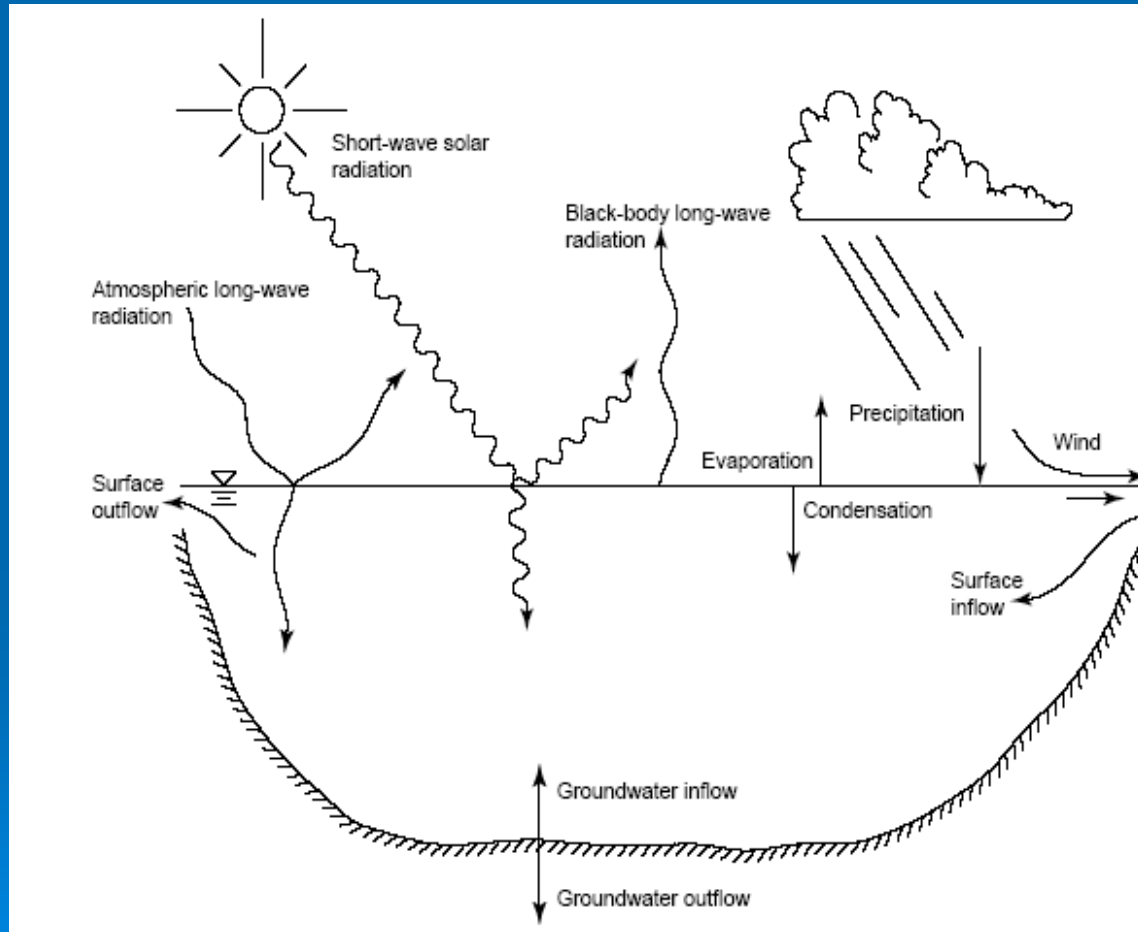


The institute covers 3,500 hectares of land, has a closed area of about 132,000 square meters.

# Why study lakes?

- Lakes are important for their recreational, and scenic qualities, and the water they contain is one of the most treasured natural resources. Lakes constitute important habitats and food resources for aquatic life, but lake ecosystems are fragile. Lake ecosystems can undergo rapid environmental changes, often leading to significant declines in their recreational, and aquatic ecosystem functions.
- The condition of a lake at a given time is the result of the interaction of many factors—its watershed, climate, geology, human influence, and characteristics of the lake itself. With constantly expanding databases and increased knowledge, limnologists and hydrologists are able to better understand problems that develop in particular lakes, and further develop comprehensive models that can be used to predict how lakes might change in the future.

# Characterizing The Dynamical Regimes Of a Lake



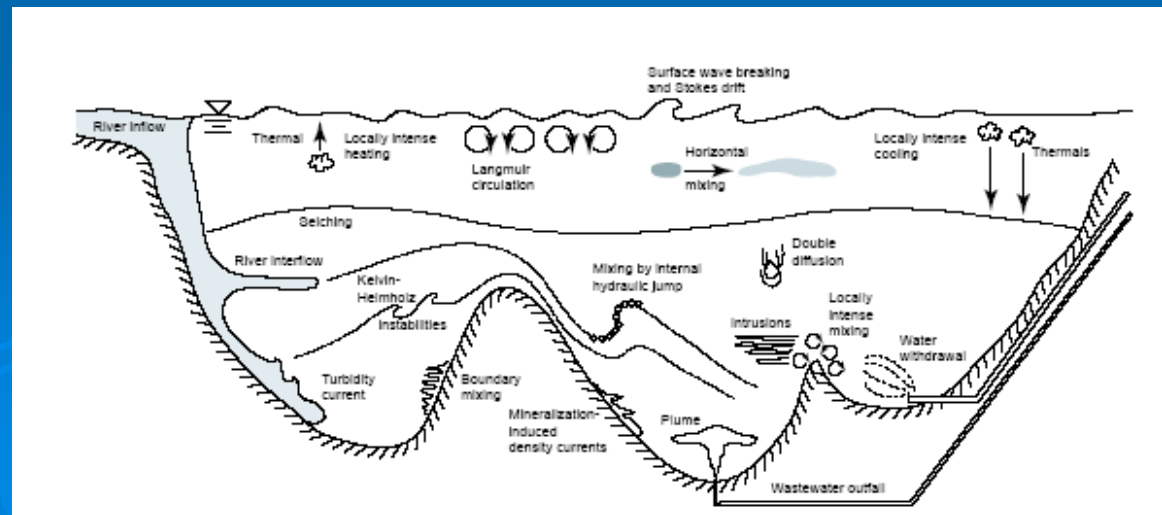
Major energy inputs to a typical lake:

- Wind
- Direct inflows and outflows
- Radiation
- Evaporation and condensation

# Major energy inputs to a typical lake: Wind

Wind is the major external input responsible for mixing.

- Wind adds kinetic energy to the lake. It imparts shear on the water surface. Shear drags water in the downwind direction adding KE and causing surface currents and waves and a so-called surface set up: the mean lake surface downwind is tilted upward compared to the upwind side of the lake. This set up results in a basin-scale circulation.
- When the wind stops, basin-scale internal waves, called seiches, which also result in boundary currents and boundary mixing. basin-scale circulation forms as the bottom water must flow upwind to satisfy mass conservation.
- Wind generates local currents that, as a result of the lake boundaries, also induce basin-scale motions.
- Near the lake surface wind is responsible for surface waves and surface currents.
- Wave breaking enhance gas exchange with the atm.
- Wave breaking enhance gas exchange with the atm.
- Langmuir circulation: wind causing the formation of cells of rotating water with floating debris that is parallel to the surface.

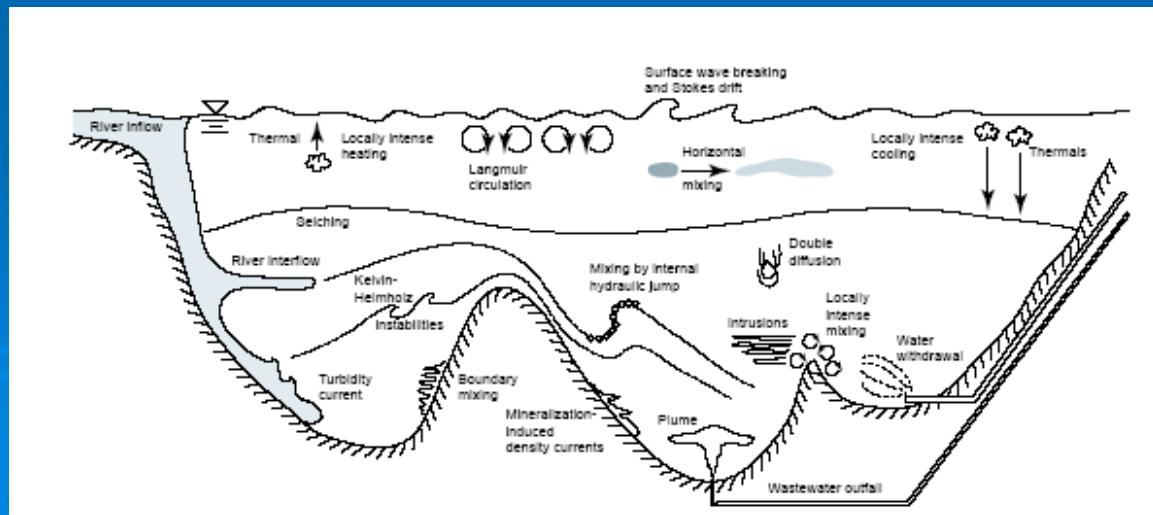




# Major energy inputs to a typical lake:

## Direct inflows and outflows

- Direct inflows to lakes and reservoirs can include: surface inflow (rivers and streams), groundwater inflow, and precipitation. Outflows from the lake can be surface or groundwater outflow. Each flow is accompanied by a heat flux.
- Inflows and outflows create mixing through their own kinetic energy and through an input of buoyancy. River inflows that are more dense than the surface water plunge to a level of neutral buoyancy and form internal currents, called intrusions.
- When river inputs contain high suspended solids or stir-up the bottom sediments, turbidity currents may develop. Turbidity currents are density currents formed by suspended particulate flows.



# Major energy inputs to a typical lake:

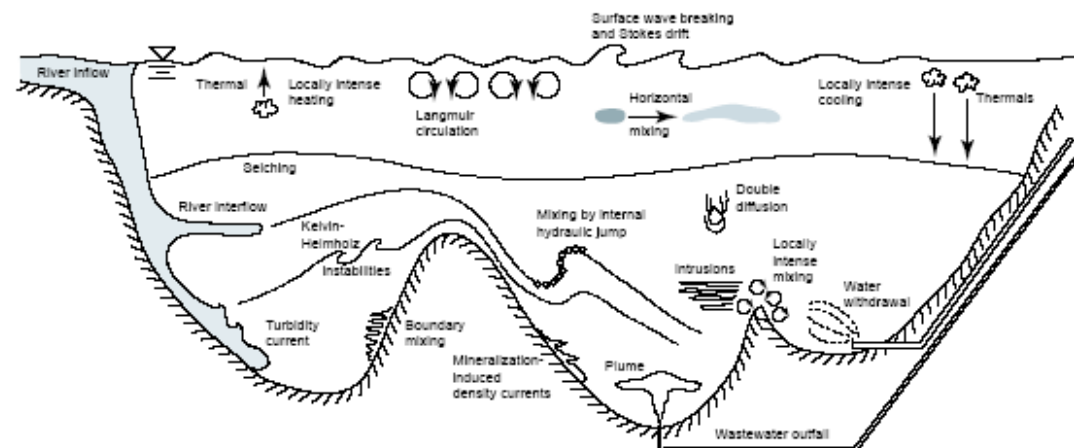
- **Radiation:** Two major types of radiation play a role in lake and reservoir stratification: short-wave ultraviolet radiation and long-wave infrared radiation.

*short-wave ultraviolet radiation:* originates from the sun. Radiation penetrating is absorbed in the water column and converted to heat.

Blue travels the farthest, it heats the deepest layers and can also travel full circle and escape from the lake, thereby, giving the lake its blue appearance.

*long-wave infrared radiation:* originates from black body radiation. Radiation emitted by the lake results in loss of thermal energy.

- **Radiation** causes mixing when an unstable density gradient is generated. For example, when suspended particles, such as algae, in the water column concentrate the solar radiative heating in a certain water layer, this region may become warmer than the water above. Warmer bottom water must rise forming a *thermal convection current*



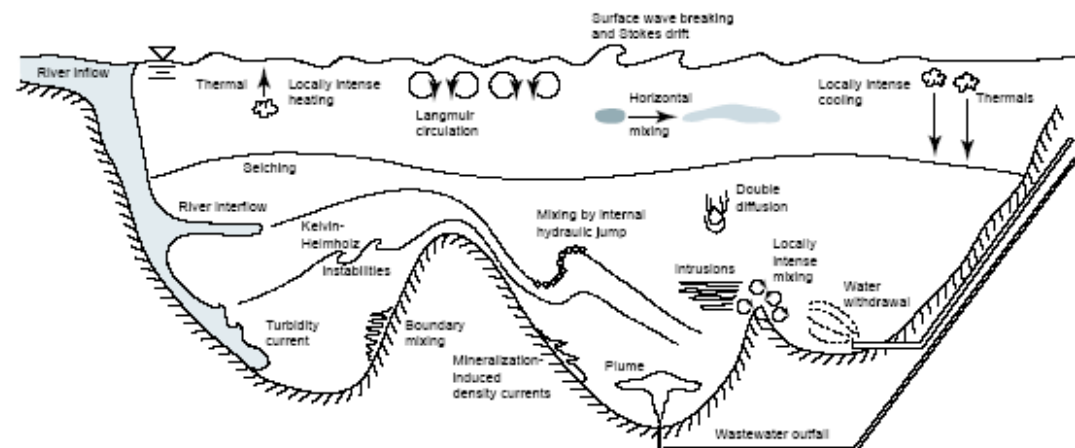
# Major energy inputs to a typical lake:

- **Evaporation and condensation:**

Evaporation: conversion of liquid water to water vapor; extracts heat from the lake cooling the water surface.

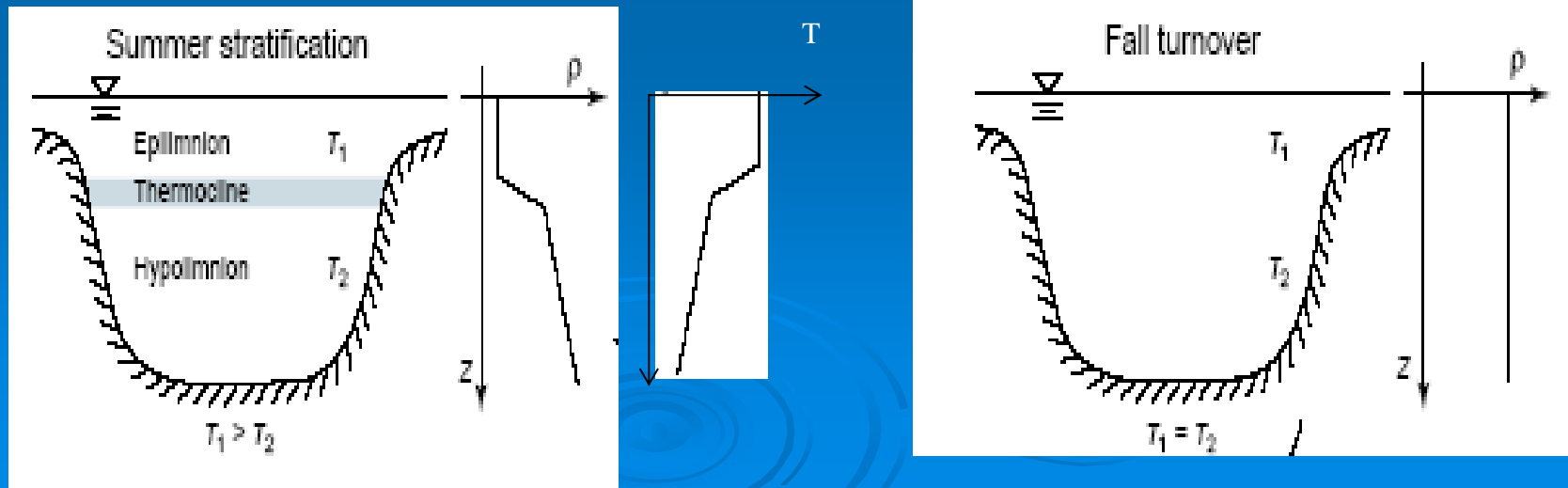
Condensation: conversion of water vapor to liquid water; extracts heat from the atm.heating the water surface.

- **Kevin Helmholtz instabilities:** In a stratified lake, gravity waves can propagate on the interface separating two layers. If layers flow at different velocities when a shear is present, waves grow in time. Internal waves (billows) generate mixing- called K-H instability.



# Thermal Stratification in Lakes

- In the summer, the high solar radiation input and warm air temperatures contribute to a strong thermal stratification of the lake. Surface water is warmer than bottom water. Winds tend to keep the surface water mixed, and this upper mixed region of the lake is called the epilimnion.
- Below the mixing action of the wind and the penetration depth of the solar radiation, a strong temperature and accompanying density gradient develops. This region of strong gradients is called the thermocline, or sometimes pycnocline. Below the thermocline a weaker temperature gradient is observed and the water is cool and comparatively quiescent. The bottom region of the lake is called the hypolimnion.

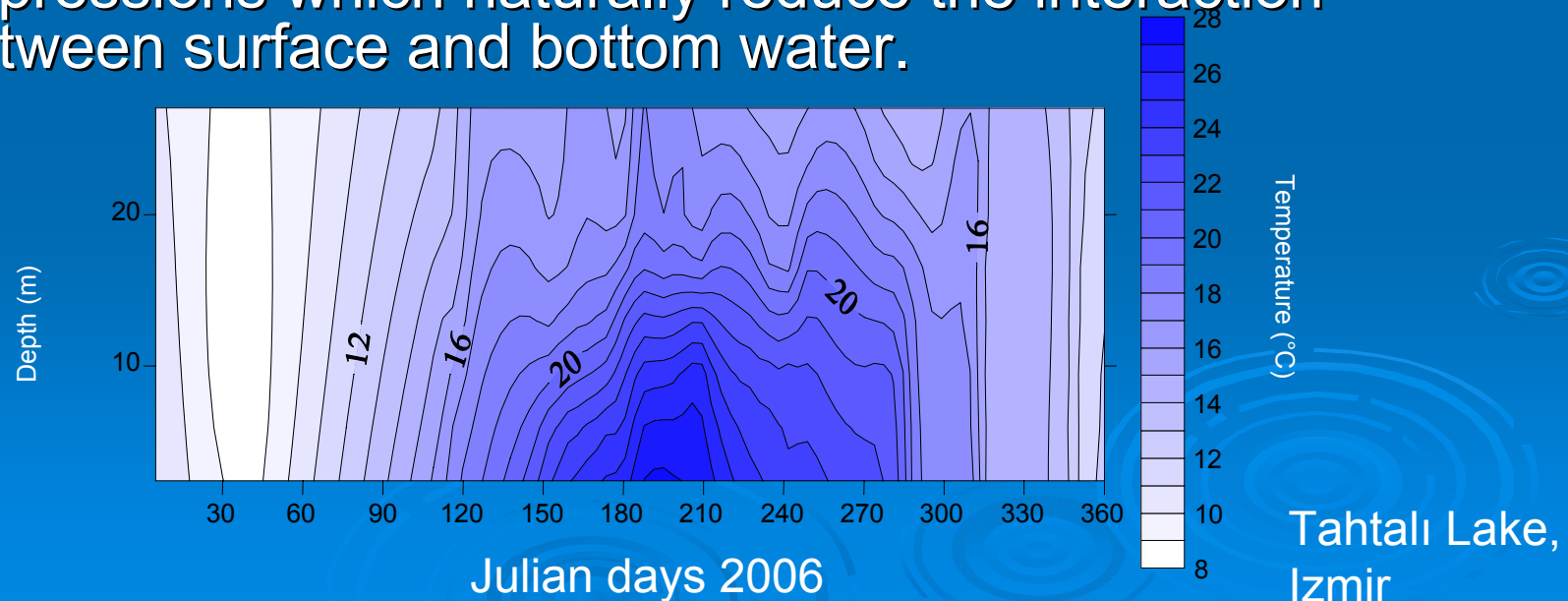


# Thermal Stratification in Lakes

Stratification reduces vertical exchange in lakes.

Lakes and reservoirs are stratified for three main reasons:

- 1. Lakes and reservoirs are comparatively stagnant, having low velocities, often laminar in nature.
- 2. Lakes and reservoirs have long residence times (retention time).
- 3. Lakes and reservoirs form in (sometimes deep) depressions which naturally reduce the interaction between surface and bottom water.



# Lake mixing regimes

- A question of great ecological importance is whether meteorological conditions are such as to cause the surface layer to stratify or mix at a particular instant in time. This may be answered by comparing the magnitude of the *rate of working of the wind* with *the rate at which thermal energy adds potential energy* to the surface water column.



# Lake mixing regimes, Richardson number

- A non-dimensional number that expresses the mixing potential of a shear flow in a stably stratified ambient is the Richardson number, Ri.
- Ri gives the ratio of the stability due to the stratification compared to the instability caused by the wind stirring

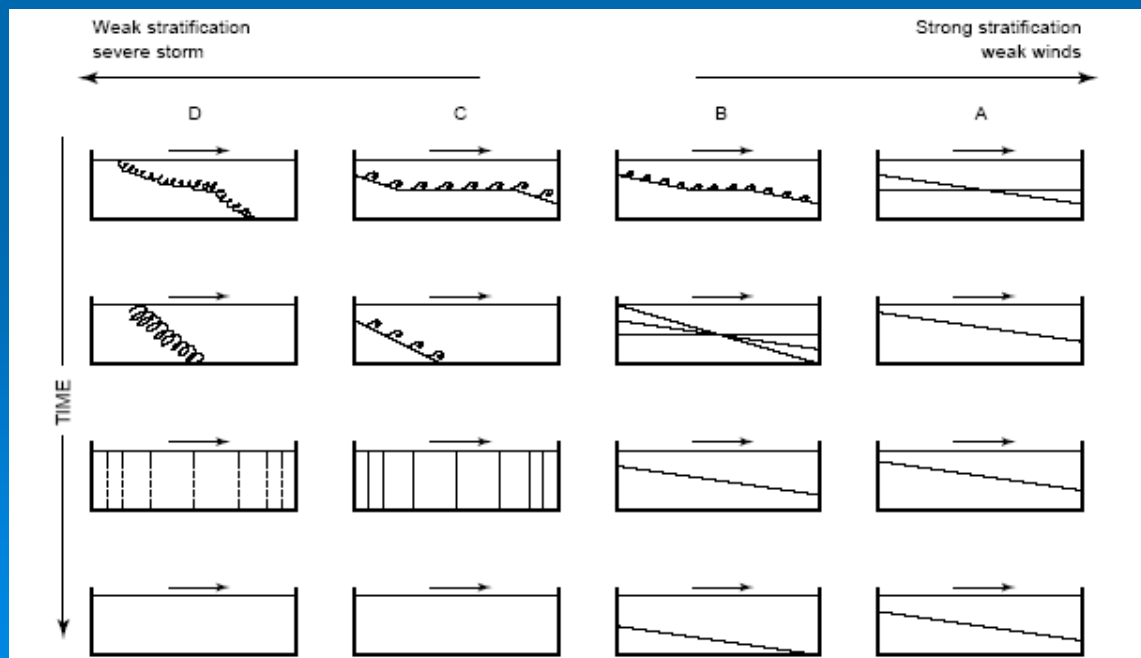
$$u_* = \left| 0.0013 \frac{\rho_a}{\rho_w} U_{10}^2 \right|^{1/2}$$

$$g' = g \frac{(\rho_h - \rho_e)}{\bar{\rho}}$$

$$Ri_* = \frac{g' \bar{h}}{u_*^2}$$

# Lake mixing regimes, Richardson Number

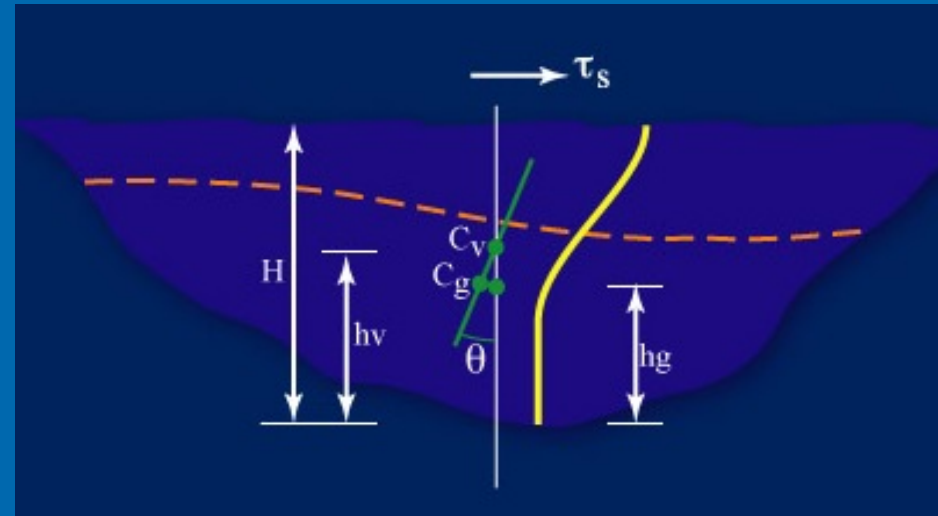
- **Regime A:**  $Ri > L^2/(2h)^2$  The deepening process proceeds very slowly by turbulent erosion.
- **Regime B:**  $L/(2h) < Ri < L^2/(2h)^2$  Internal waves are the predominant feature of this regime. Entrainment and billowing have minor effects on the internal waves, yet the wave amplitude can be quite severe. Erosion keeps the interface sharp and it is energized almost exclusively by surface stirring.
- **Regime C:**  $1 < Ri < L/(2h)$  Throughout this regime the thermocline will be diffuse and steeply inclined. The process deepens the epilimnion rapidly to the bottom, the mixing being predominantly energized by shear production.
- **Regime D:**  $Ri < 1$  Deepening is now so rapid and chaotic that the interface will not be well defined.





# Lake mixing regimes, Lake Number

- Imberger (1998) also characterized the hydrodynamic regimes in a lake through dimensional analysis. He defined a non-dimensional parameter (Lake Number), in terms of the total depth of the lake, the height from the bottom of the lake to the seasonal thermocline, the height to the center of volume of the lake, the surface area of the lake, the shear velocity, and the stability



Moments about  $C_v$

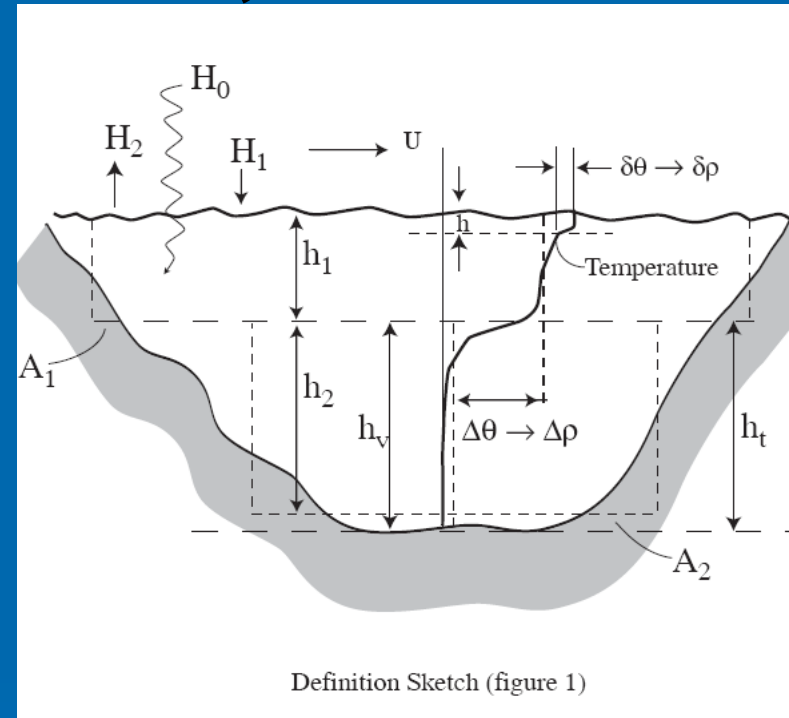
$$\curvearrowright M_N = \rho u_*^2 A_S (H - h_v)$$

$$\curvearrowleft M_g = M_g (h_v - h_g) \sin \theta$$

$$\text{Ratio} \quad \frac{M_g}{M_w} \Big|_{\text{upwelling}} = L_N = \frac{S_t (H - h_t)}{u_*^2 A_S^{3/2} (H - h_v)}$$

# Lake mixing regimes, Lake Number

- $LN < 1$  upwelling occurs.
- $1 < LN < 3$  indicate partial upwelling, and boundary mixing may occur.
- $LN \gg 1$  stratification is strong



$$L_N = \frac{S_t (H - h_T)}{u_*^2 A_s^{3/2} (H - h_v)}$$

$$S_t = \frac{1}{\rho_0} \int_0^H g (h_v - z) \rho(z) A(z) dz \cong \frac{1}{2} \left( \frac{\Delta \rho}{\rho} g \right) \frac{A_1 A_2 h_1 h_2 (h_1 + h_2)}{(A_1 h_1 + A_2 h_2)}$$

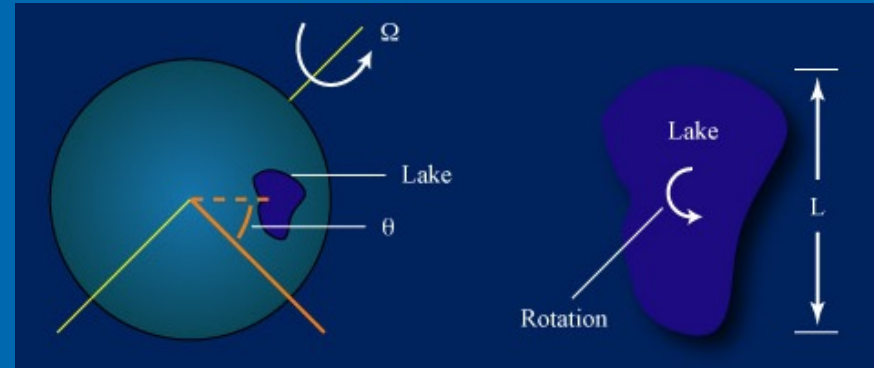
# The Effect of Earth's Rotation

- In large lakes the earth's rotation is often important and may influence the motion in the lake. A particle travelling in a straight line relative to the rotating lake must be experiencing a force, the Coriolis force.
- *Importance of the earth's rotation is defined by Burger's Equation:*

$$S_i = \frac{c_i}{Lf}$$

$$f = \Omega \sin \theta$$

the ratio of time of travel of an internal wave across the lake  $L/c_i$ , where  $c_i$  is phase speed of the wave, and  $L$  the size dimension of the lake, to the time it takes for the lake to rotate about its axis  $1/f$ , where  $f$  is the inertial frequency at the latitude of the lake.



When  $S_i < 1$

the earth's rotation dominates the dynamics and the waves have the character of an inertial oscillation with most of the energy in the wave being kinetic energy.

When  $S_i > 1$  the internal oscillations progressively take on the characteristics of simple gravitation seiches.

# River Inflow Dynamics

- Whether a flow separation occurs as the river enters the lake may be answered by noting that the internal Froude number  $Fr_i$  of an underflow is constant,

$$Fr_i = \frac{u_i}{(g_i' D)^{1/2}} = \frac{Q_i}{(g_i' D)^{1/2} A_i}$$

$$g_i' = \left( \frac{\Delta\rho_i}{\rho_0} \right) g$$

- $\Delta\rho_i$  is the difference in density between the inflowing water and the surface water,  $D$  is the hydraulic radius of the underflow and  $A_i$  is the inflowing area. Suppose  $B$  represents the width of the lake, then  $D = A_i/B$  and  $A_i \sim HB$  so that if  $h_i$  is the depth at which point the inflow becomes an under- or overflow then

$$\frac{h_i}{H} = \left( \frac{Q_i}{g_i'^{1/2} H^{3/2} B} \right)^{2/3} Fr_{ic}^{2/3}$$

where  $Fr_{ic}$  is the critical value of the plunge ( $Fr_{ic} = 1$ )

# River Outflow Dynamics

- In man made reservoirs, if water is withdrawn from an outlet at small discharges, the vertical density gradient may produce buoyancy forces sufficiently strong to prohibit extensive vertical motions so that the water withdrawn comes from a thin horizontal layer at the level of the intake. At somewhat larger discharges the withdrawal layer may intersect the thermocline and at very large discharges the effects of buoyancy may be completely overwhelmed and the flow returns to potential flow (Fischer et al. 1979), where equipotential lines are perpendicular to streamlines which are tangent to the velocity vector of the flow.
- Ivey and Blake (1985) outflow dynamics at the outlets were investigated via transition number
- If  $S > 3$  the inertia-buoyancy regime governs the flow,

$$S = \left( Q^2 N \nu^{-3} \right)^{1/15}$$

# River Outflow Dynamics

- Wood and Binney (1976) examined lowering of upper water layer (drawdown) into a line sink positioned in the lower layer, suggesting the use of Froude number to define the critical discharge at which the drawdown occurs. Two cases may be defined for the radial flow. First, the outlet is close to the bottom of the lake and second, the outlet may be very much closer to the thermocline.

$$F_{3c} = \frac{Q_{3c}}{\left[ \left( \frac{\Delta\rho + \alpha^2 \Delta^1\rho}{\rho_0} \right) g d^5 \right]^{1/2}} = 1.02$$

$$d \approx (H - h)$$

$$F_{3c} = 2.04$$

$$d \ll (H - h)$$

- where;  $\Delta\rho$  is the density difference between the water at the surface and at the thermocline;  $\alpha^2$  is the density jump coefficient;  $\Delta^1\rho$  is the density difference between the water at the offtake and that at the top of the hypolimnion;  $d$  is the distance between the center of the outlet and the layer interface.

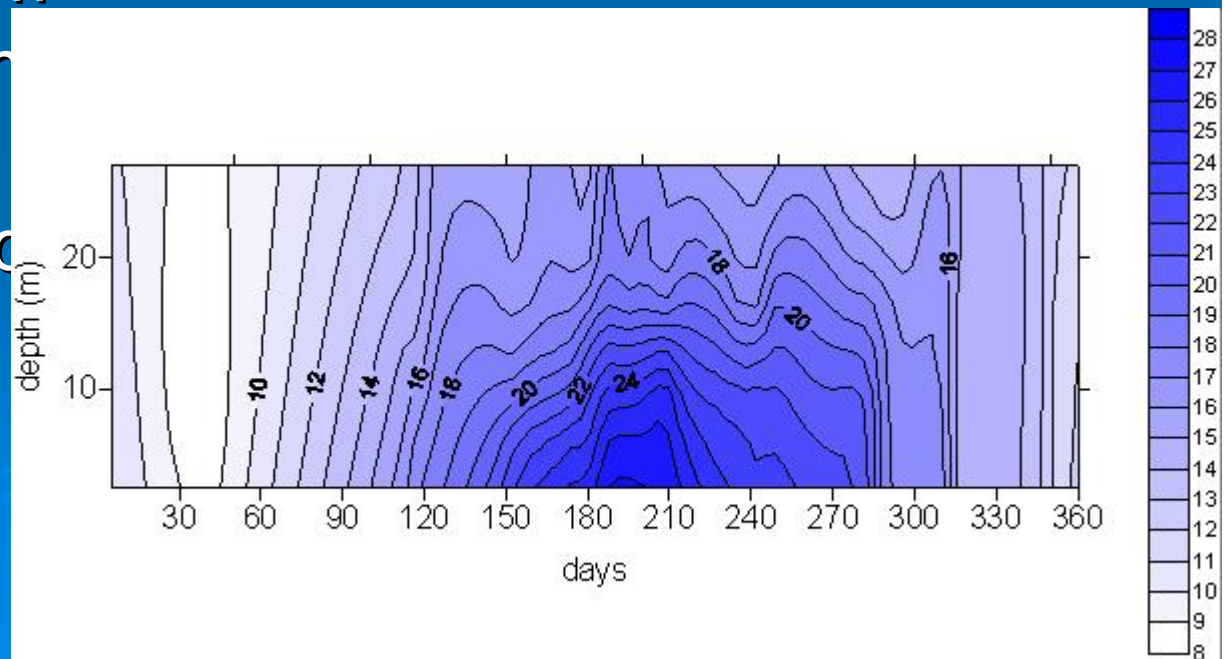
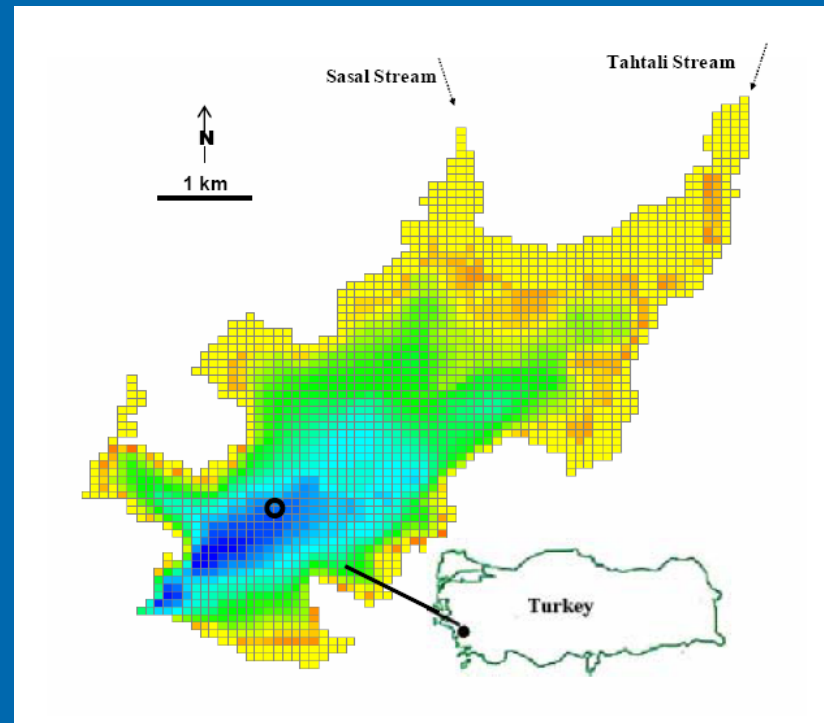
# Case Study: Effects of thermal stratification and mixing on reservoir water quality

- Two projects funded by research grants from European Commission and Tubitak
- Projects involve:  
**Investigation of the Effects of Thermal Stratification on Hydrodynamics of a Reservoir**
- Monthly field trips to a reservoir from June to December 2006
- Synchronized water quality and flow measurements



# Study Site

- completed in 1997
- capacity of the dam : 175 million m<sup>3</sup>
- average water: 1.9 lt/s
- surface area : 18 km<sup>2</sup>
- mean depth : 15 m
- max. depth : 22 m
- wind : NE
- thermally stratified in summer





# Motivation

- Stratification during the summer acts as a barrier restraining mixing of the water column. The warm water in the epilimnion is unable to move through the cold, dense water of the hypolimnion. As a result of incomplete mixing of the water column and lack of light for the photosynthesis at the hypolimnion, the water column can become anoxic.
- This study was motivated by the degradation of water quality in the summer because of thermal stratification, as observed in many reservoirs and lakes around the world. Tahtali Lake, providing 40% of its fresh water to Izmir, Turkey, was selected as study site, because the lake experienced dense stratification during the summer months leading to deterioration of water quality.

# Methodology : Nondimensional analysis

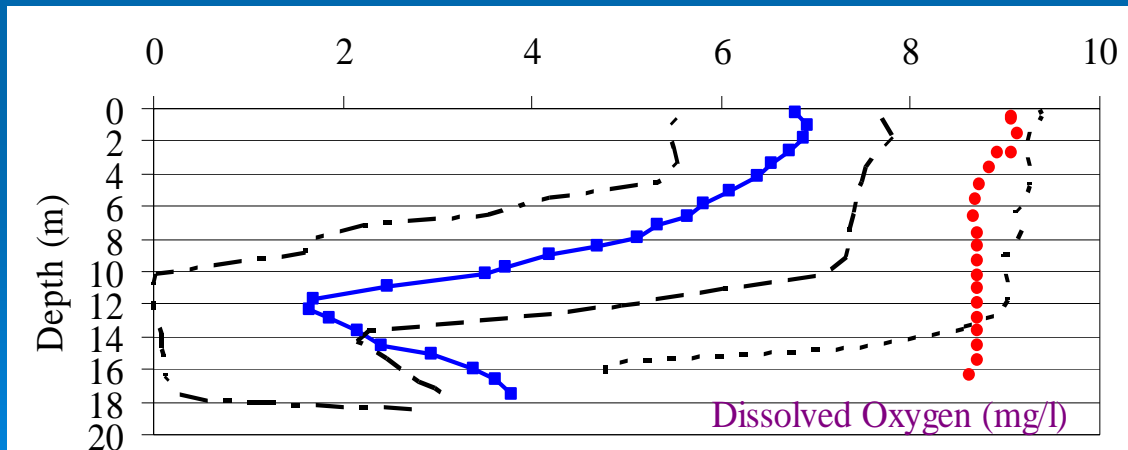
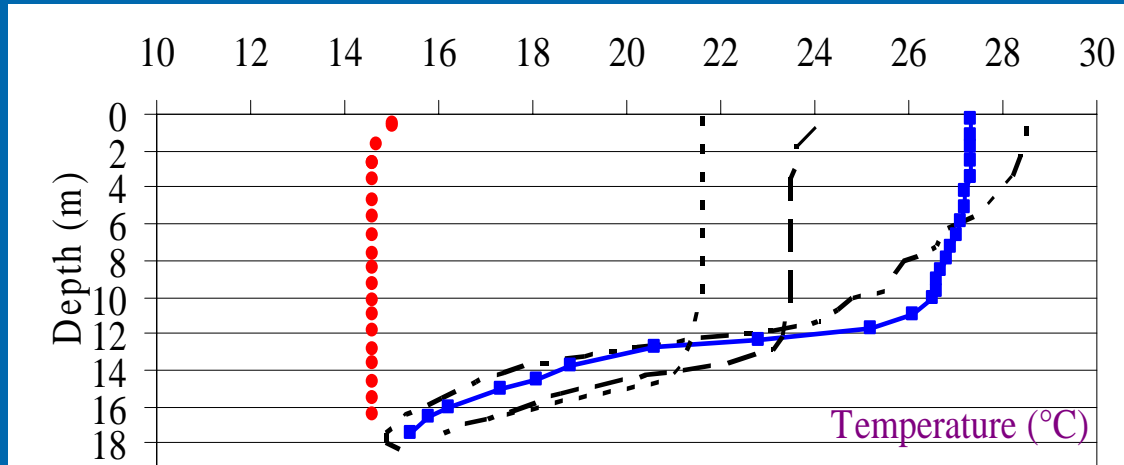
- **Nondimensional analysis** conducted to determine if the stratification is dominant
- *Lake Number (LN)* was calculated for the conditions in August, October, and November 2006. The critical value for stratification was found to be 3 based on water quality measurements. The wind speed corresponding to this value was calculated as 3 m/s for Tahtali Reservoir. In August, LN was smaller than the critical value 18% of the time, which indicates dense stratification in the lake. However, in October, this value increased to 33% and in November reached a value of 100% indicating that the lake was no more stratified beginning from November.
- In Lake Toolik, Alaska/USA, the lake was stable with 1 m/s wind speed as it was in Tahtali Reservoir. However, the wind speed required for upwelling was 7 m/s for Lake Toolik (MacIntyre et al.2006). In another study on Lake Tahoe, the critical wind speed for upwelling was estimated 4 m/s (Schladow and Thompson 2000). The critical value of LN is reached in Lake Hartwell when the wind speed was 18 m/s, suggesting stronger stratification.
- **Water Quality Measurements**
- **Statistical Analysis**

# Methodology : Water Quality Measurements



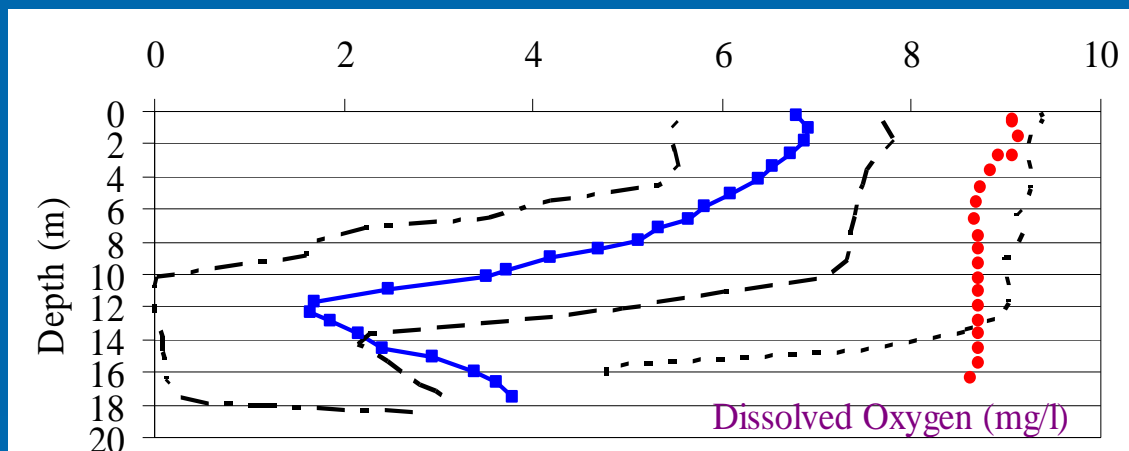
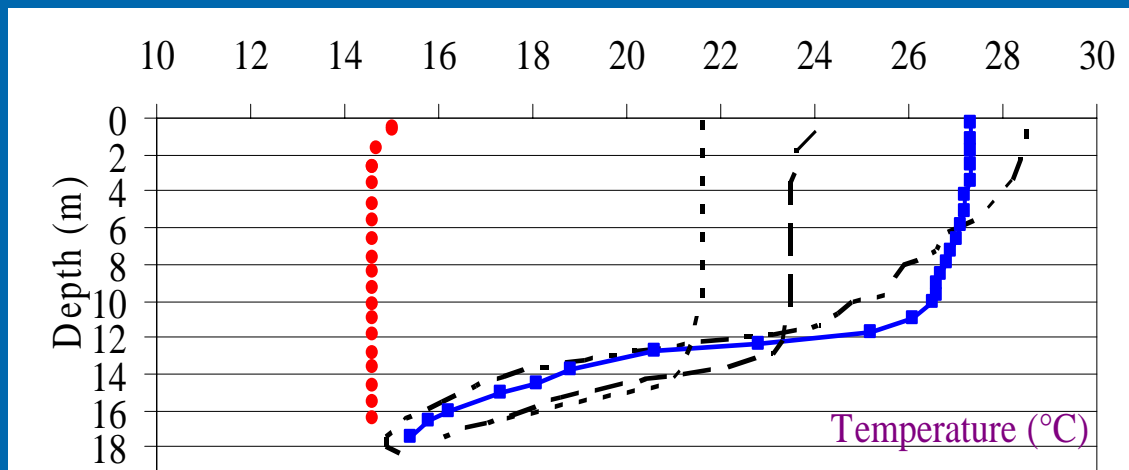
DKK-TOA's multiparameter water quality meter (measuring temperature, DO, pH, turbidity, conductivity) was used. Water quality data were recorded at 1-m intervals in the vertical. Time series measurements of water temperature and water quality data were recorded at 30-min intervals.

# Methodology : Water Quality Measurements



- Stratification was evident in August where water temperature at the surface reached 28 ° C and the thermocline started at a depth of 10 m.
- In October, however, surface temperatures decreased to 21.5 ° C and the thermocline moved to a depth of 14 m, indicating mixing of most of the water column.
- In November, the temperature profile was uniform throughout the water column at 15 ° C.

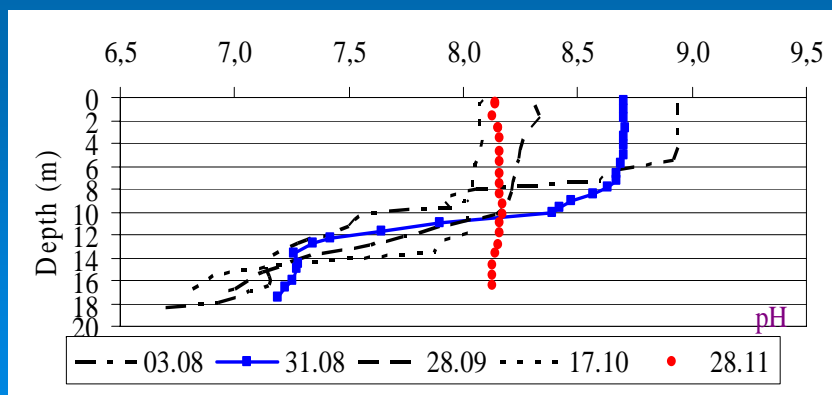
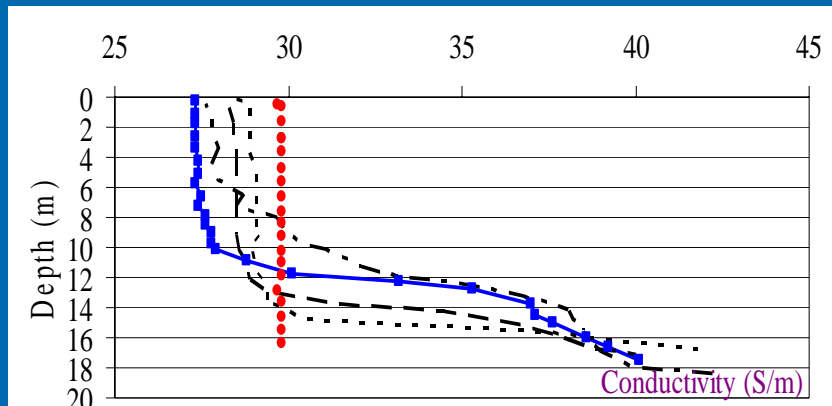
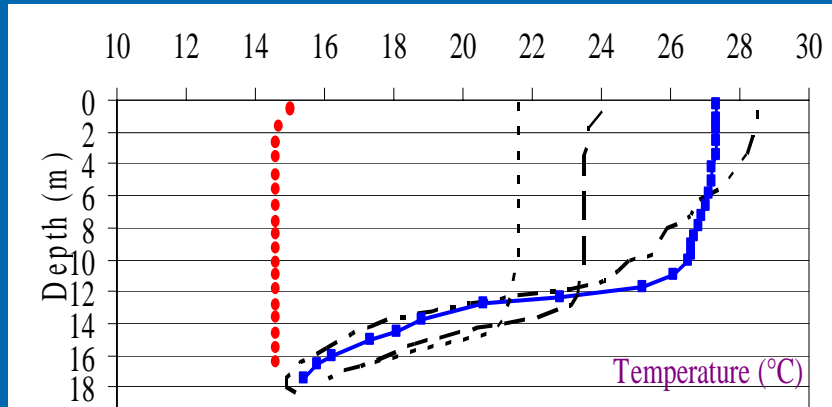
Red : 28/11 Blue 31/8



Observed DO values dropped well below the standard limit of 5 mg l<sup>-1</sup> at the thermocline, leading to the development of anoxia during the summer period. This can partly be explained by sinking of organic material produced in the epilimnion to the thermocline, where oxidization reduces the DO in the thermocline.

Red : 28/11 Blue 31/8

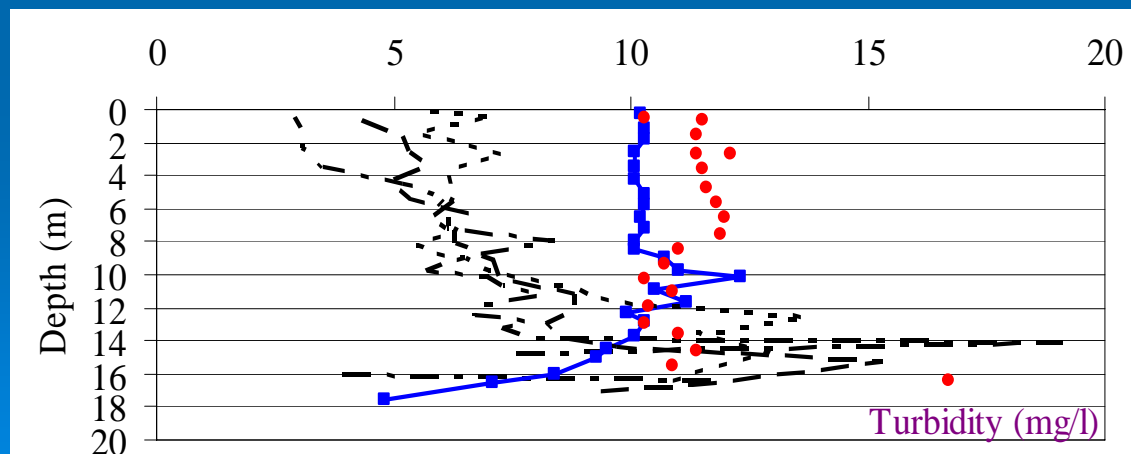
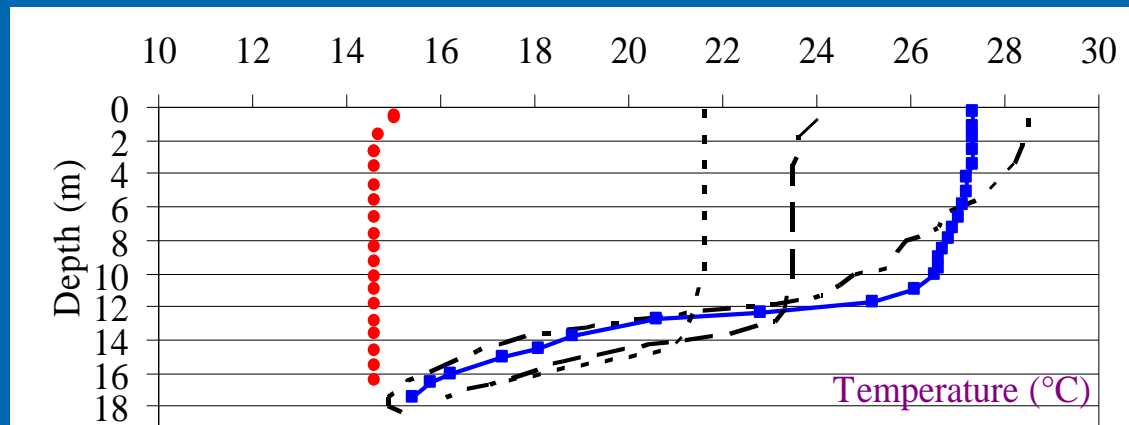
As mixing was induced during the fall by the decrease of air temperature, and thus water temperatures at the epilimnion, an increase in DO values at the epilimnion were observed while deepening of the level of maximum DO proceeded until it reached the bottom. In November, the DO profile was uniform throughout the water column at 9 mg l<sup>-1</sup>. The increase in the DO concentration below the thermocline observed in August was attributed to convective circulation introduced by lateral flow from side arms of the lake.



A decrease in pH in the lower layers of the stratified lake was observed due to accumulation of  $\text{CO}_2$ , because no light could penetrate through the thermocline to the hypolimnion during the summer period and plants could not consume  $\text{CO}_2$  by photosynthesis. Furthermore,  $\text{CO}_2$ , released as a result of decomposition of organic matter in the hypolimnion dissolves in water to form carbonate ions, increasing the ion concentration.

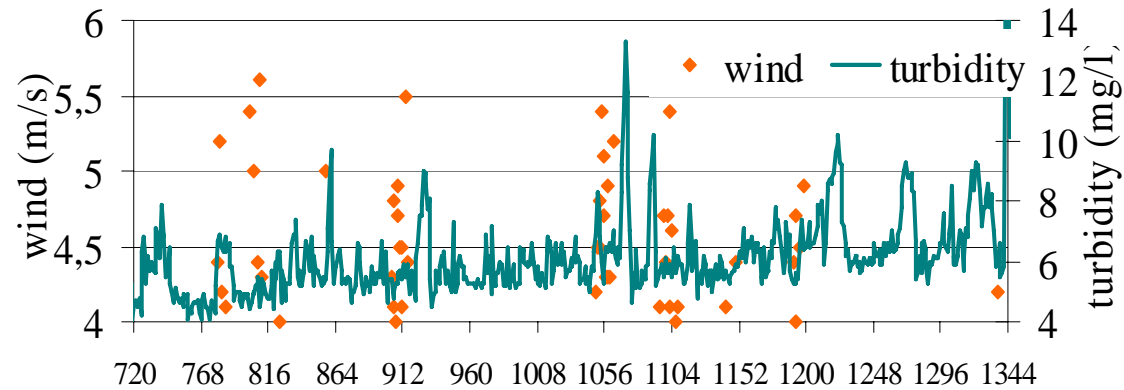
This increase in the ion concentration was reflected as an increase of electrical conductivity measured in the hypolimnion during the summer period. In November, the pH and the electrical conductivity profiles were uniform.

# Methodology : Water Quality Measurements

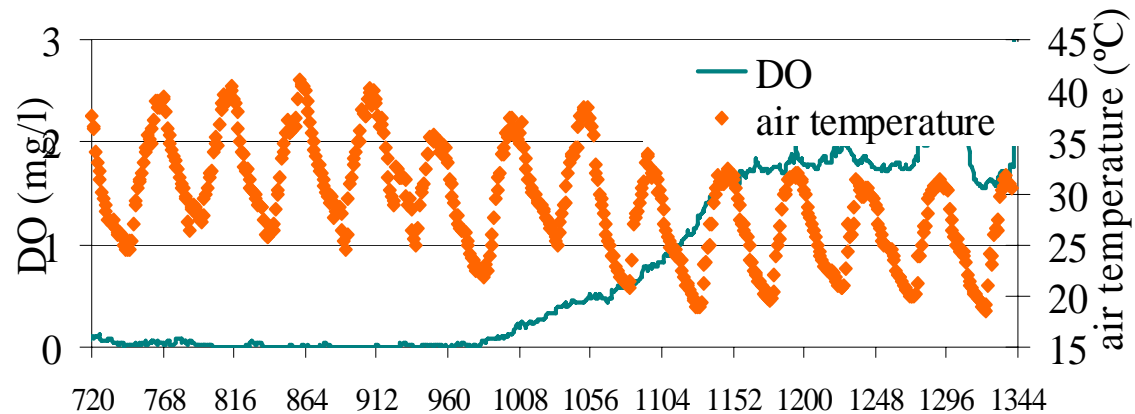


Turbidity peaks are found mostly in the thermocline region. Turbidity increases are closely related to the location of the maximum density gradient in the vertical, where low turbulence is expected because of stabilization of the water column. A noticeable increase in turbidity toward the bottom of the lake on 17.10.06 was probably because of the effect of the relatively cold sediment-laden water flowing into the lake after a rain event.

# The variation of recorded DO and turbidity time series with air temperature and wind speed in August 2006



data # for August 2006 (48 data = 1day)

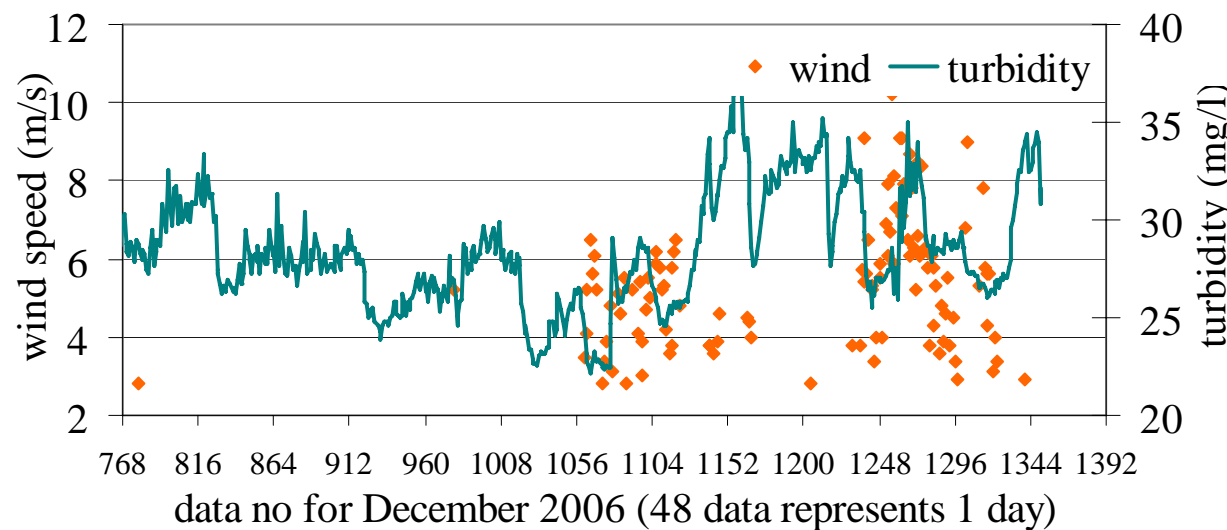
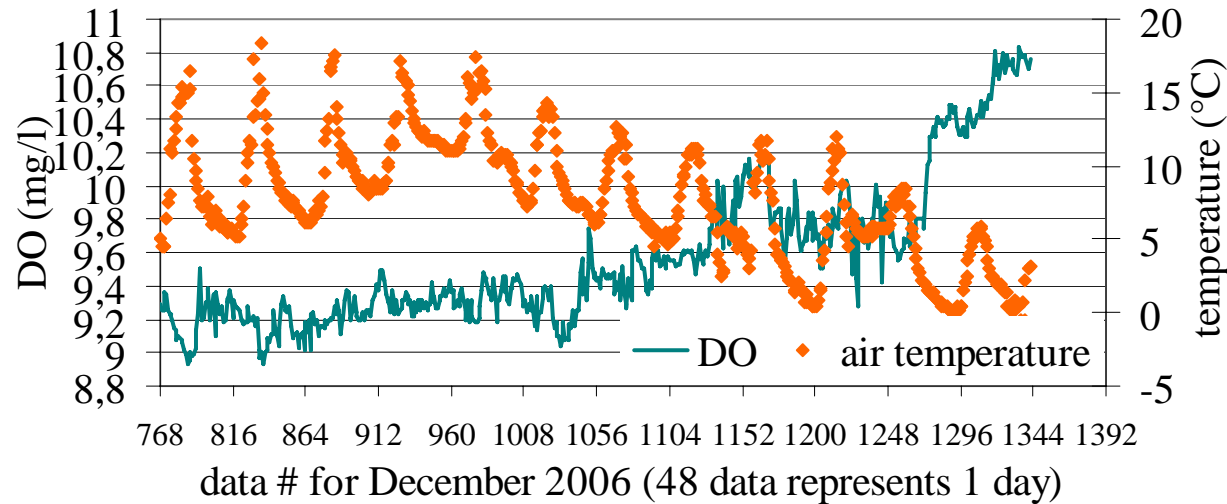


data # for August 2006 (48 data = 1day)

*The water quality meter was left at the depth of ~11 m (thermocline).*



## The variation of recorded DO and turbidity time series with air temperature and wind speed in December 2006

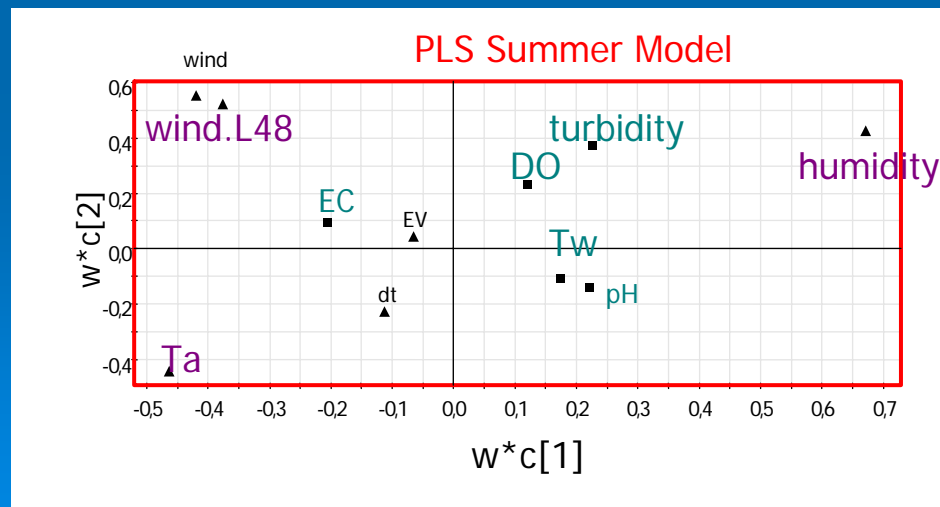
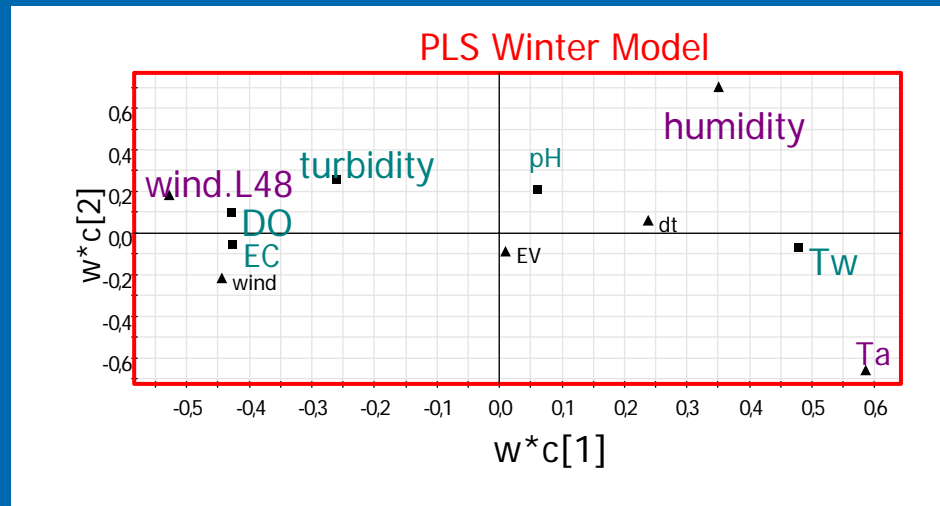


*The water quality meter was left at the depth of ~11 m (thermocline).*

# Statistical Analysis

- Multivariate analysis was carried out on a data matrix of seven variables (air temperature, wind speed, wind direction, lagged wind speed, humidity, evaporation, and temperature difference).
- The purpose of this analysis was to determine which of these variables were influential in modelling water-quality parameters such as pH, conductivity, DO, and turbidity.
- Rainfall data were excluded from the analysis, because it rained only twice during the period of the observations and thus data were insufficient to include in the analysis. Wind-speed data were lagged by 24 h, and 24-h differences in air temperatures were included in the model.
- Models developed by principal-component analysis (PCA), and partial least-squares (PLS) analysis expressed the correlations between different variables which were used to identify the most influential variables.
- Simca-P 10.5 software (Umetrics 2003) was applied for PCA and PLS modelling.

# Statistical Analysis



According to the results from PLS analysis, in winter, air temperature and one-day-lagged wind speed were the most dominant variables affecting observed dissolved oxygen and turbidity values. However, in summer and in fall, humidity and air temperature were the most dominant variables.

# Statistical Analysis

- Results of the statistical analysis showed that air temperature, lagged wind speed, and humidity are the influential parameters affecting variations in water-quality parameters. Therefore in such analysis the non-dimensional parameters water temperature and wind alone do not suffice, and variations in water quality structure should be evaluated by new approaches considering other meteorological factors.

# Hydrodynamics of Lakes and Reservoirs

Advanced techniques for measurement  
of flow, bathymetry and sediment in  
lakes: Focus on acoustic techniques

ERASMUS LECTURES PREPARED FOR  
LUND UNIVERSITY

**Assoc.Prof.Dr.ŞEBNEM ELÇİ**

IZMIR INSTITUTE OF TECHNOLOGY

CIVIL ENGINEERING DEPT.

# Historical Measurements:

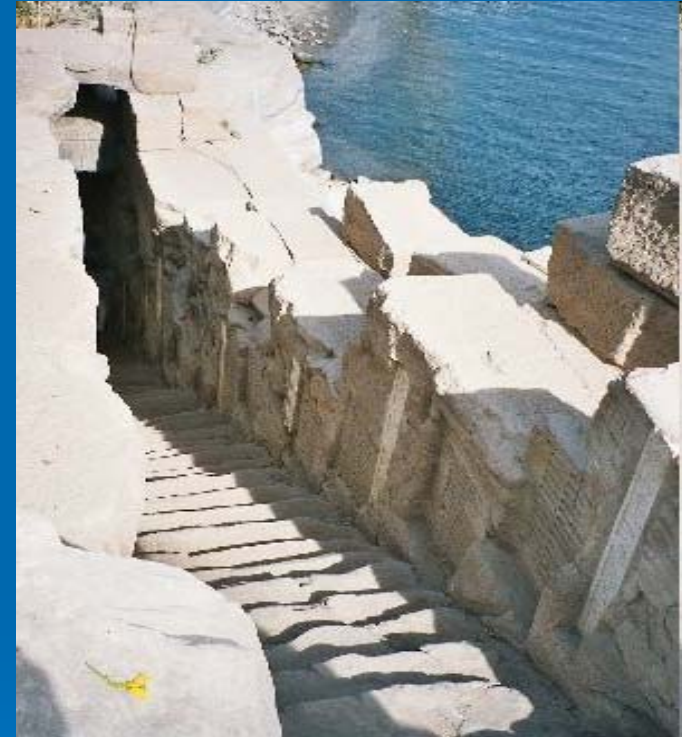
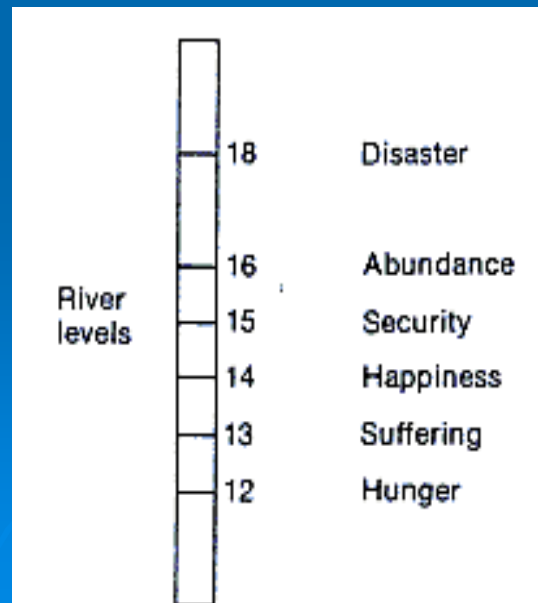
## Mesopotamia and Egypt

- The first successful efforts to control the flow of water were made in Mesopotamia and Egypt (5800 B.C.), where the remains of the prehistoric irrigation works still exist. In ancient Egypt, the construction of canals was a major endeavor of the pharaohs and their servants, beginning in Scorpio's time.



# Historical Measurements: Egypt

- The first water structures were seen in Egypt as early as 3000 B.C. The records of water levels of the Nile back to 3000-3500 B.C. The device used for measuring the water level of the Nile river during the annual flood season is called *Nilometer*.



# Historical Measurements:

## Sumerians; Assyrians

- The Sumerians in southern Mesopotamia built city walls and temples and dug canals that were the world's first engineering works. It is also of interest that these people, from the beginning of recorded history, fought over water rights.
- The Assyrians also developed extensive public works. Sargon II, invading Armenia in 714 B.C. , discovered the *qanat* (Arabic name) or *kariz* (Persian name), which is a tunnel used to bring water from an underground source in the hills down to the foothills. Sargon destroyed the area in Armenia but brought the concept back to Assyria. This method of irrigation spread over the Near East into North Africa over the centuries and is still used. Tehr also built a new canal, nearly 19 kilometers long, with an **aqueduct** that had a layer of concrete or mortar under the upper layer of stone to prevent leakage.



# Historical Measurements: Hittite period

- Anatolia, also called Asia Minor, which is part of the Republic of Turkey, has been the crossroads of many civilizations during the past 10,000 years. During the past 4,000 years, going back to the Hittite period (2000–200 B.C. ), there are many remains of ancient urban water-supply systems, including pipes, canals, tunnels, inverted siphons, aqueducts, reservoirs, cisterns, and dams.
- An example of one city is Ephesus, which was founded during the tenth century B.C. as an Ionian city out of the Artemis Temple. In the sixth century B.C., it settled in the neighborhood of the Artemis Temple. Water was supplied to Ephesus from springs at different locations. In addition, water-well cisterns supplied water to the city. Water for the great fountain, built during 4–14 A.D., was diverted by a small dam at Marnss and conveyed to the city by a 6-kilometer-long system consisting of one larger and two small clay pipelines.

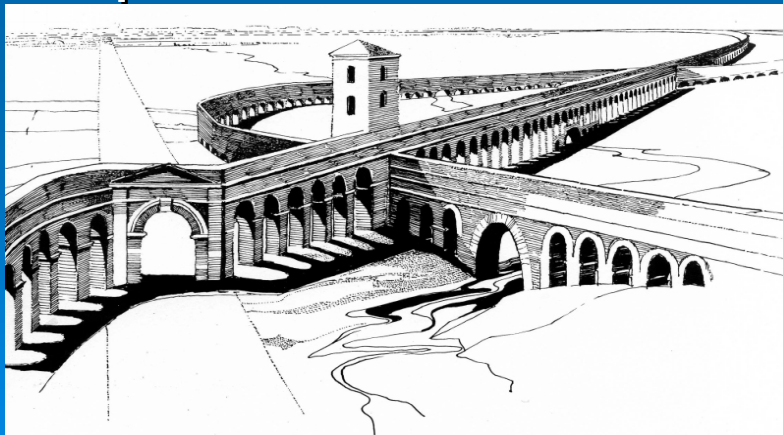
# Historical Measurements:

## *Thales; Platon; Aristoteles*

- The first philosopher accepted by history of scientists is *Thales* who lived at Miletus (624-548 B.C.). Thales is the first philosopher who proclaimed that *water is the original substance of all the things on the earth.*
- *Platon* is a well known philosopher who lived and lectured at his Academia in Athens (428-348 B.C.). He gave the explanation of hydrologic cycle saying that “rivers and springs originate from rainfall”.
- *Aristoteles* (384-322) wrote an article on hydrology entitled “*Meteorologica*”. He explained the mechanics of precipitation and gave his thoughts on winds and seas.
- The first measurement of rainfall depth was begun in India during this period. The non-recording type rain gauges were extensively used so that lands could be taxed according to the rainfall they received. (Biswas, 1969).

# Historical Measurements: Romans

- The Romans (900 B.C.- 300) were practical engineers.
- They constructed excellent aqueducts to supply millions of liters of fresh water to the city of Rome, sewerage systems which are still in use and a very fine harbor in the Western Roman Empire.



- The 1375 m long arcade of two Roman aqueducts, seen from the north

# Historical Measurements: Leonardo da Vinci

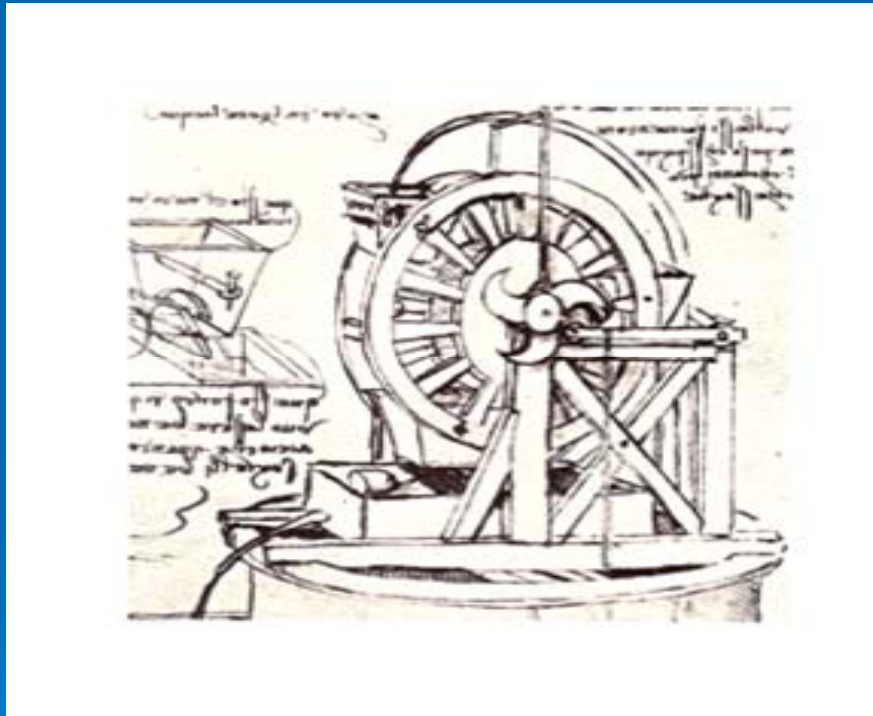
- Hero, a Greek of the first century, was the first to express the basis for flow measurement as we know it today. This important finding went unnoticed, however, for about 1500 yr until Leonardo da Vinci extended the relationship to the continuity equation, but even da Vinci's work went unknown until his manuscripts were found in 1690.

- *Leonardo da Vinci* (1452-1519) is an artist and scientist of the Renaissance era who also interested in hydrology and hydraulics.
- He made experiments to measure the velocity of flow by using floating corks.

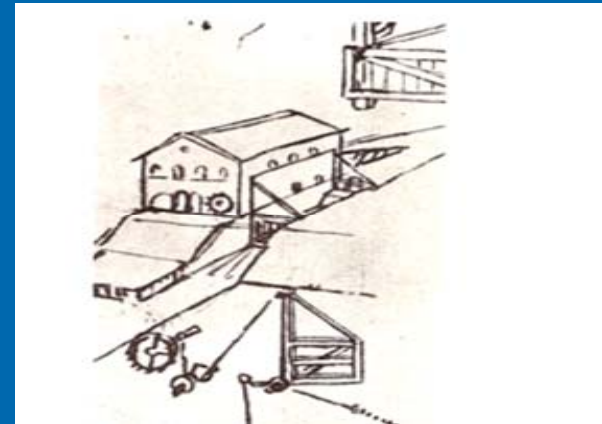


# Historical Measurements: Leonardo da Vinci

- He also developed experiments in glass wall canals to understand the principles of flow by using dye.



Water pump drawn by Leonardo  
(Hamyln,1968)



Water mill drawn by Leonardo  
(Hamyln,1968)

# Historical Measurements:

## Reinhard Woltman

- The German engineer, Reinhard Woltman, developed the spoke-vane current meter in 1790, a breakthrough for measuring velocities in rivers and canals.
- During the 18th and 19th centuries development and installation of weirs and flumes made flow measurements possible on irrigation canals, and gaging stations were constructed on many rivers to provide records of flows. New technology has provided various water measurement techniques, and stream flow data now can be accessed at over 4200 gaging stations in the U.S.

# Flow Measurement

- Mechanical flow meters
- Pressure- based meters
- Weirs
- Dye measurements
- Electromagnetic, ultrasonic flow and Laser Doppler flow meters



# Mechanical flow meters

## ➤ Bucket-and-stopwatch

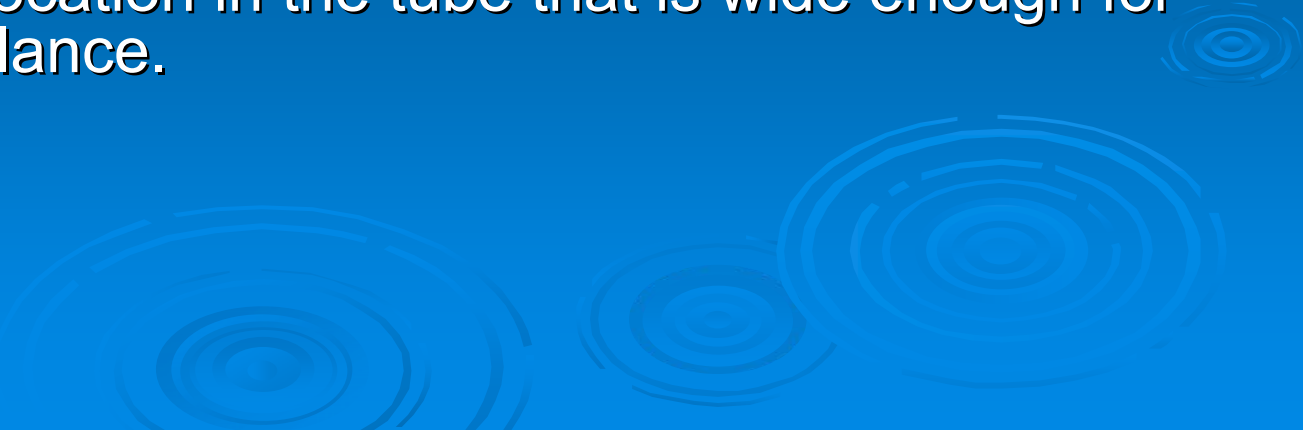
the simplest way to measure volumetric flow is to measure how long it takes to fill a known volume container.

## ➤ Piston meter

operates on the principle of a piston rotating within a chamber of known volume.

## ➤ Variable area meter

consists of a tapered tube, typically made of glass, with a float inside that is pushed up by fluid flow and pulled down by gravity. As flow rate increases, greater viscous and pressure forces on the float cause it to rise until it becomes stationary at a location in the tube that is wide enough for the forces to balance.





# Mechanical flow meters

## ➤ Turbine flow meter

turbine wheel is set in the path of a fluid stream. The flowing fluid impinges on the turbine blades, imparting a force to the blade surface and setting the rotor in motion. When a steady rotation speed has been reached, the speed is proportional to fluid velocity.

## ➤ Current meter

flow through a large penstock such as used at a hydroelectric power plant can be measured by averaging the flow velocity over the entire area.



# Pressure- based meters

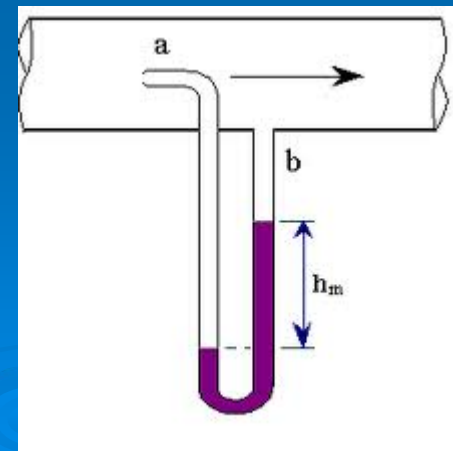
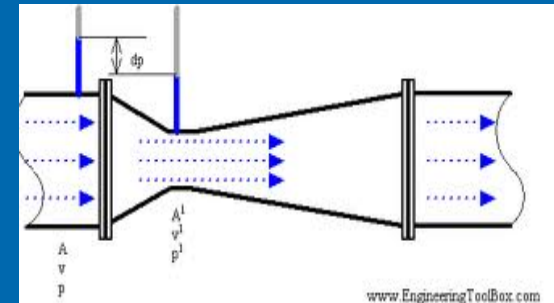
- There are several types of flow meter that rely on Bernoulli's principle, either by measuring the differential pressure within a constriction, or by measuring static and stagnation pressures to derive the dynamic pressure.

- Venturi meter

A Venturi meter constricts the flow in some fashion, and pressure sensors measure the differential pressure before and within the constriction.

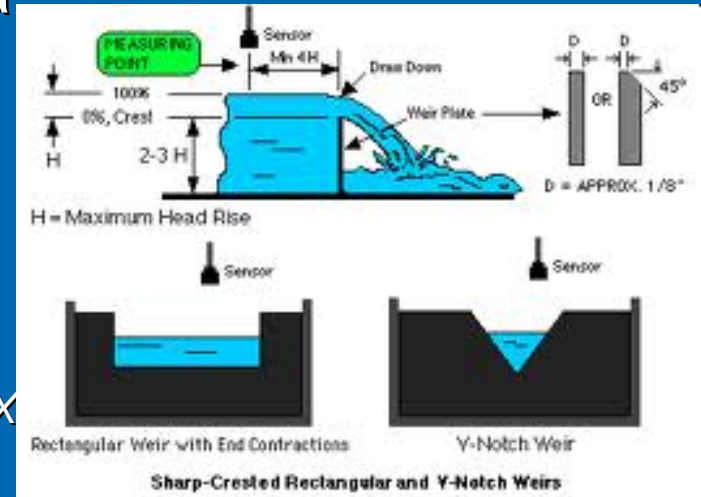
- Pitot tube

It is a pressure measuring instrument used to measure fluid flow velocity by determining the stagnation pressure. Bernoulli's equation is used to calculate the dynamic pressure and hence fluid velocity.



# Weirs; Dye measurements

- Open channel flow measurement
- The level of the water is measured at a designated point behind a hydraulic structure (a weir or flume) using various means (bubblers, ultrasonic, float, and differential pressure are common methods). This depth is converted to a flow rate according to a theoretical formula of the form  $Q = KH^X$  where  $Q$  is the flow rate,  $K$  is a constant,  $H$  is the water level, and  $X$  is an exponent which varies with the device used;
- Dye testing A known amount of dye (or salt) per unit time is added to a flow stream. After complete mixing, the concentration is measured. The dilution rate equals the flow rates.



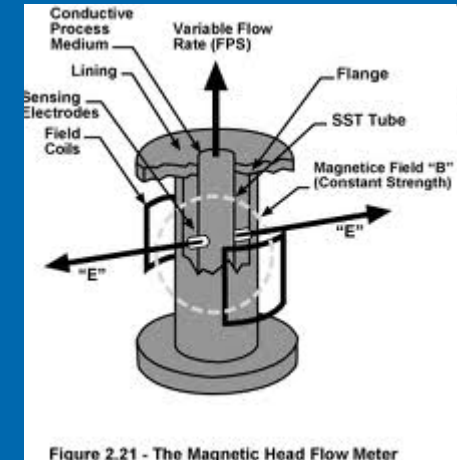
# Electromagnetic and ultrasonic flow meters

## ➤ Magnetic flow meters

A magnetic field is applied to the metering tube, which results in a potential difference proportional to the flow velocity perpendicular to the flux lines. The physical principle at work is Faraday's law of electromagnetic induction.

## ➤ Ultrasonic flow meters

They measure the difference of the transit time of ultrasonic pulses propagating in and against flow direction. This time difference is a measure for the average velocity of the fluid along the path of the ultrasonic beam.



# Doppler effect

- In his work, Austrian physicist Christian Doppler postulated his principle (1842) ([Doppler effect](#)) that the observed frequency of a wave depends on the relative speed of the source and the observer, and he tried to use this concept for explaining the colour of binary stars.



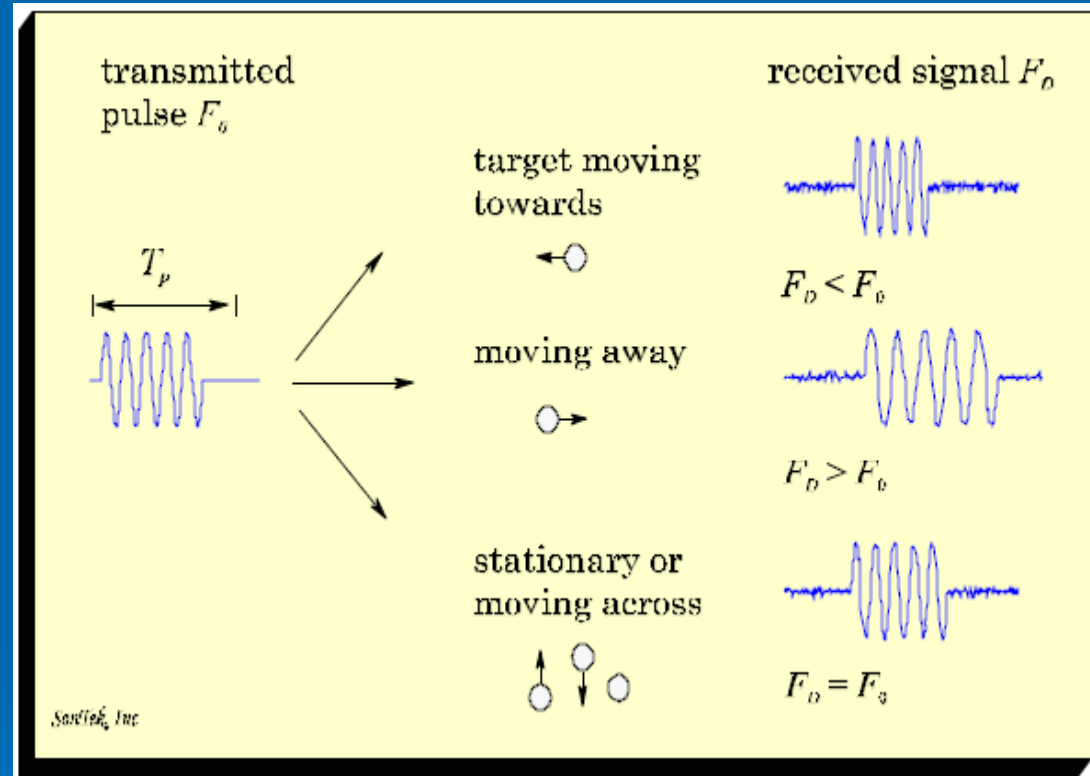
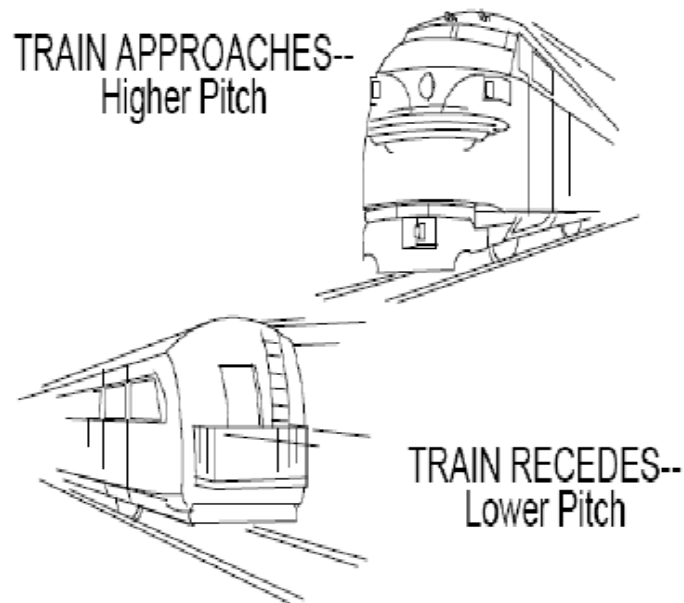
Waves emitted by a source moving from the right to the left. The frequency is higher on the left (ahead of the source) than on the right.





# Acoustic Doppler Current Profilers (ADCP) : Principles of Operation

## Doppler Shift When a Train Passes



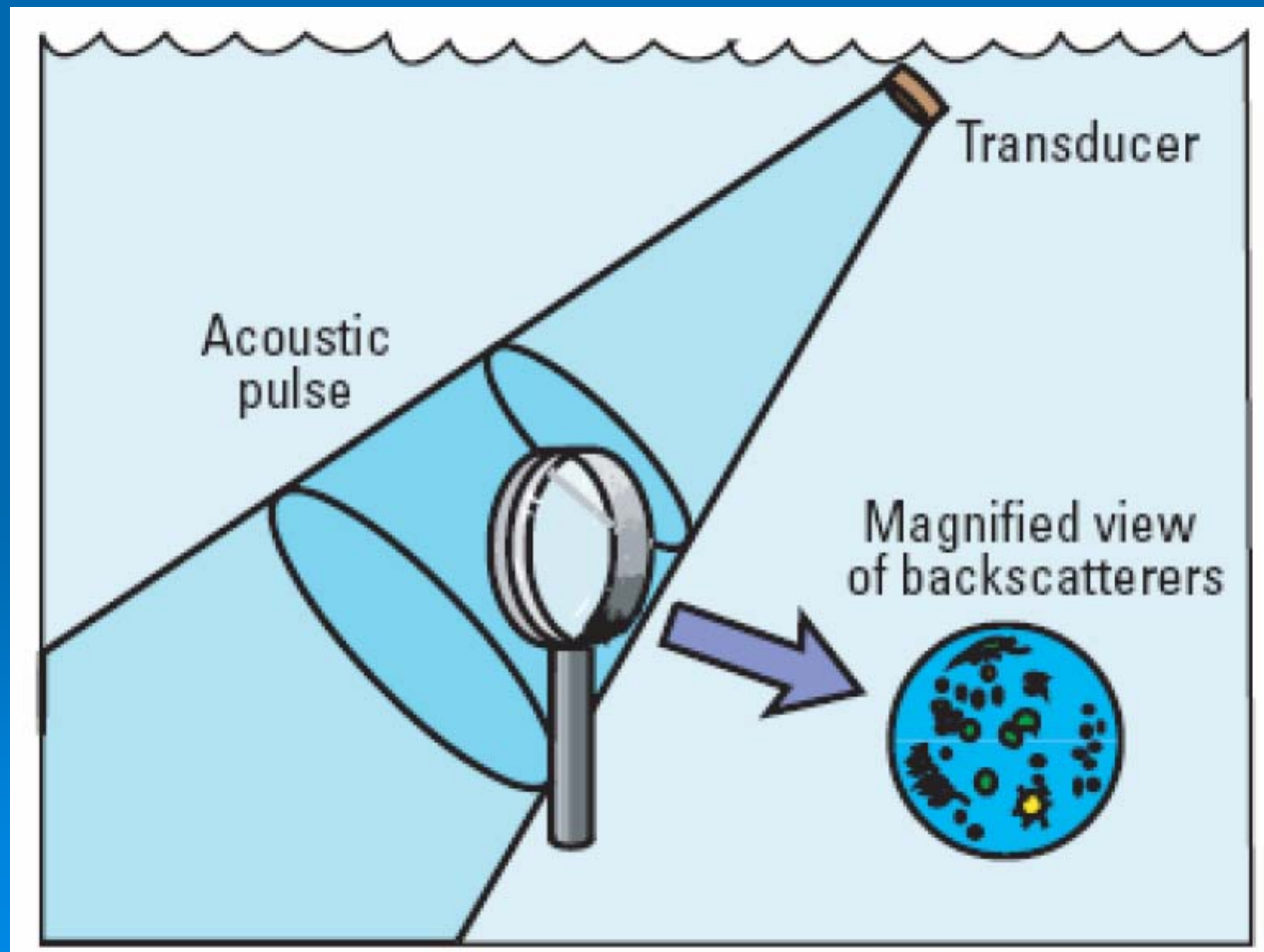
## Doppler Shift for Reflected Sound

$F_{\text{doppler}}$  : change in received frequency  
(Doppler shift)  
 $F_{\text{source}}$  : frequency of transmitted sound  
 $V$  : relative velocity of particles  
 $C$  : speed of sound

$$F_{\text{doppler}} = -2F_{\text{source}} \frac{V}{C}$$

# Acoustic Doppler Current Profilers (ADCP) : Principles of Operation

The sound pulse is reflected by **suspended particles** in the water column





**Signal-to-Noise Ratio (SNR):** function of the amount and type of particulate matter in the water.

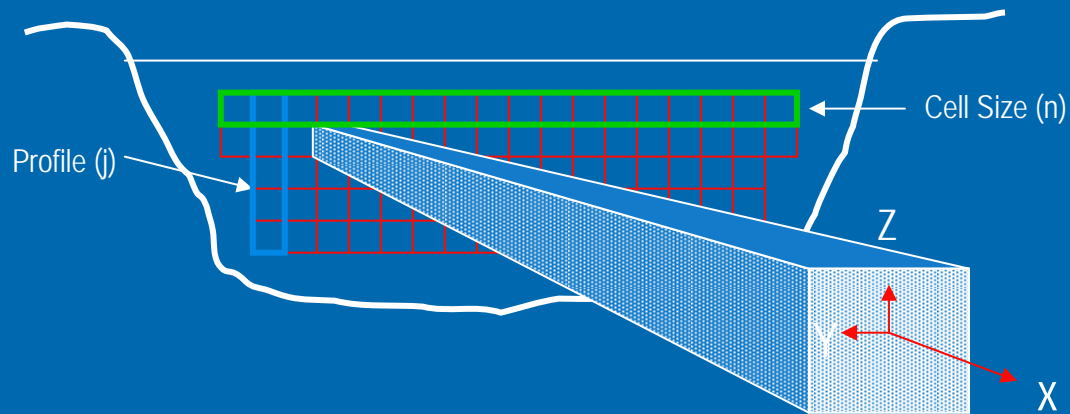
Doppler systems rely on small particles (sediment, small air bubbles, organisms, etc.) to reflect a fraction of the transmitted acoustic energy back to the transducers.

- SNR is the ratio of signal intensity (the actual reflections from particles in the water) to noise intensity.
- For making “good” measurements requires min. SNR=10 db

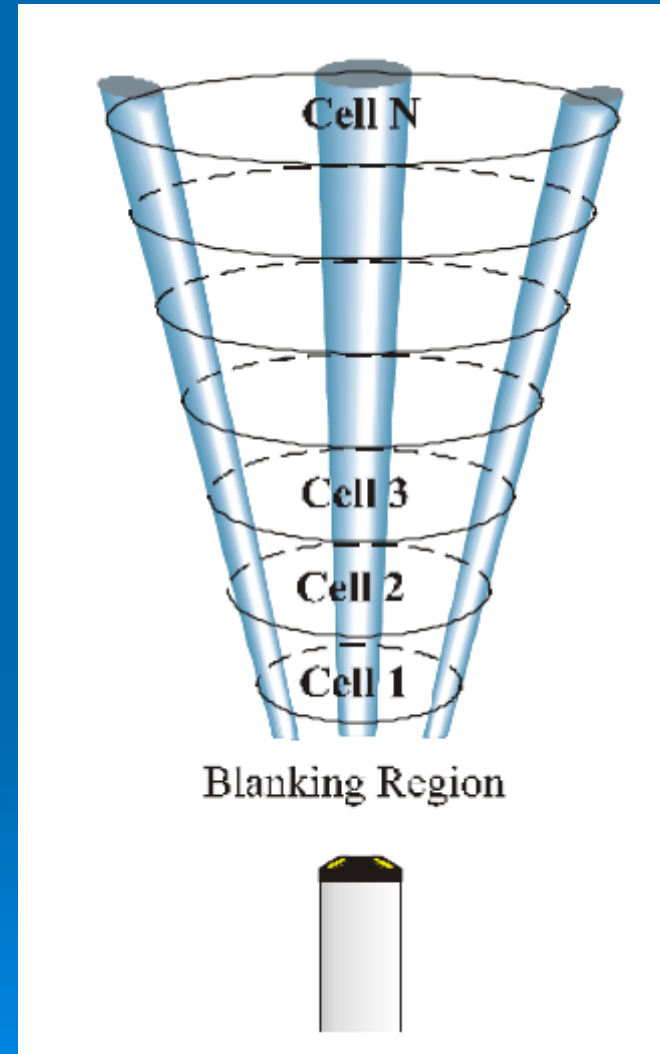
**Sound Speed :** ADCP uses sound speed (SSP) to compute velocity from the measured Doppler shift, and to precisely determine the location of the sampling volume. The SSP in water is primarily a function of temperature and salinity.

- A temperature change of 5°C results in a SSP change of ≈1%.
- A salinity change of 12 ppt results in a change in SSP of ≈1%.
- A 1% error in SSP results in a ≈2% error in velocity data

# Cell Size

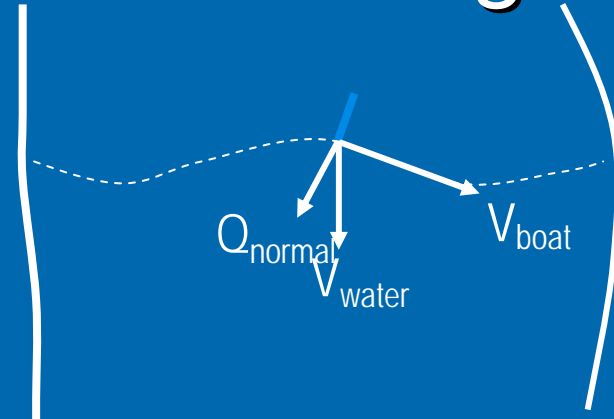


The cell size specifies the vertical range over which the signal returns are averaged for each depth cell.

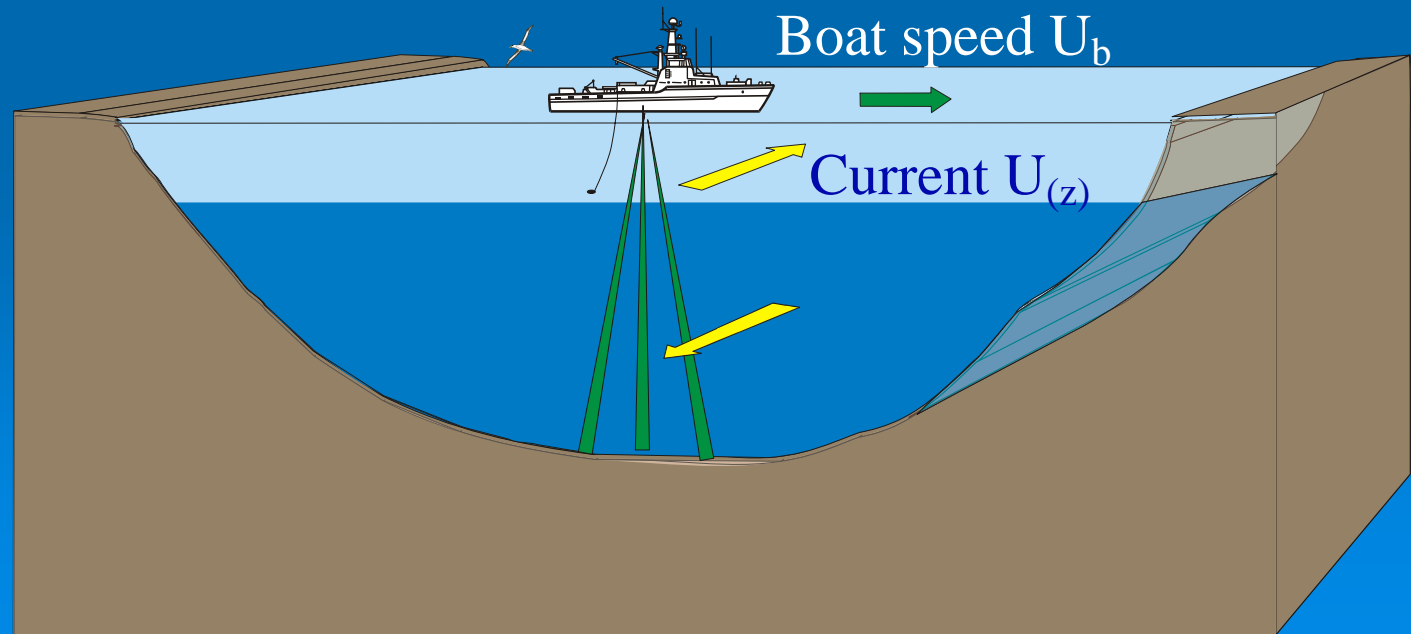


# How does ADCP's compute discharge ?

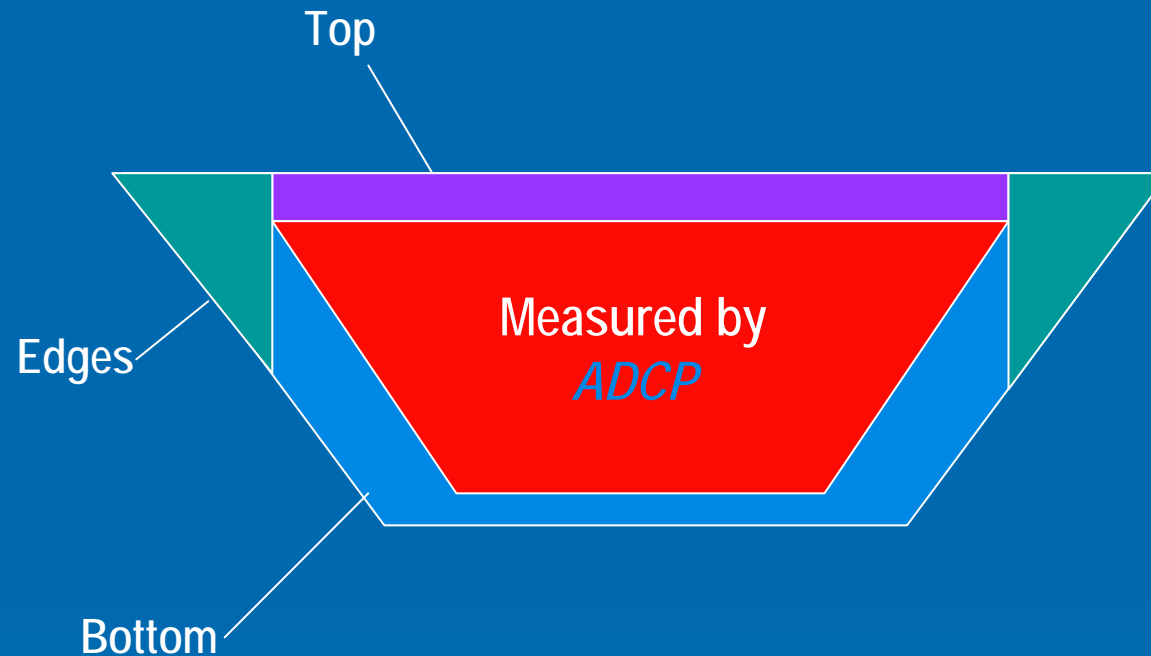
- Discharge is summed as the vessel crosses the river from bank to bank.
- Discharge can be measured over a changing course.
- It accounts for boat speed and direction.



Measured Current:  $U_m = U_b + U_{(z)}$



# How does ADCP's compute discharge ?



*'Unmeasured sections'* are estimated using the the Software

# Discharge Measurement Principle

## 1. General Equation for Total Discharge:

$$Q = \int_s \overline{V}_f \cdot \overline{n} ds$$

$V_f$  = Mean water velocity vector

$n$  = Mean unit vector normal to “ $ds$ ”

$ds$  = Differential area

## 2. Taking into account ADP provides vessel-velocity and water-velocity:

$$Q_t = \int_0^T \int_0^d (\overline{V}_f \times \overline{V}_b) \cdot \overline{k} dz dt$$

*After Christensen and Herrick, 1982*

$T$  = traverse time,

$d$  = total depth,

$V_b$  = Mean vessel velocity,

$k$  = unit normal vector in “ $z$ ” dir.

$dz$  = vertical differential depth

$dt$  = differential time

# Discharge Measurement Principle

$$Q_m = \sum_{i=1}^{N_s} \left[ \int_0^{d_i} (V_{xm} V_{by} - V_{ym} V_{bx})_i \cdot dz \right] t_i$$

*after Christensen and Herrick, 1982*

$N_s$  = Number of subsections (profiles),

$i$  = subsection,

$d$  = depth of subsection,

$V_{xm}$  = x-component of mean measured water-velocity vector,

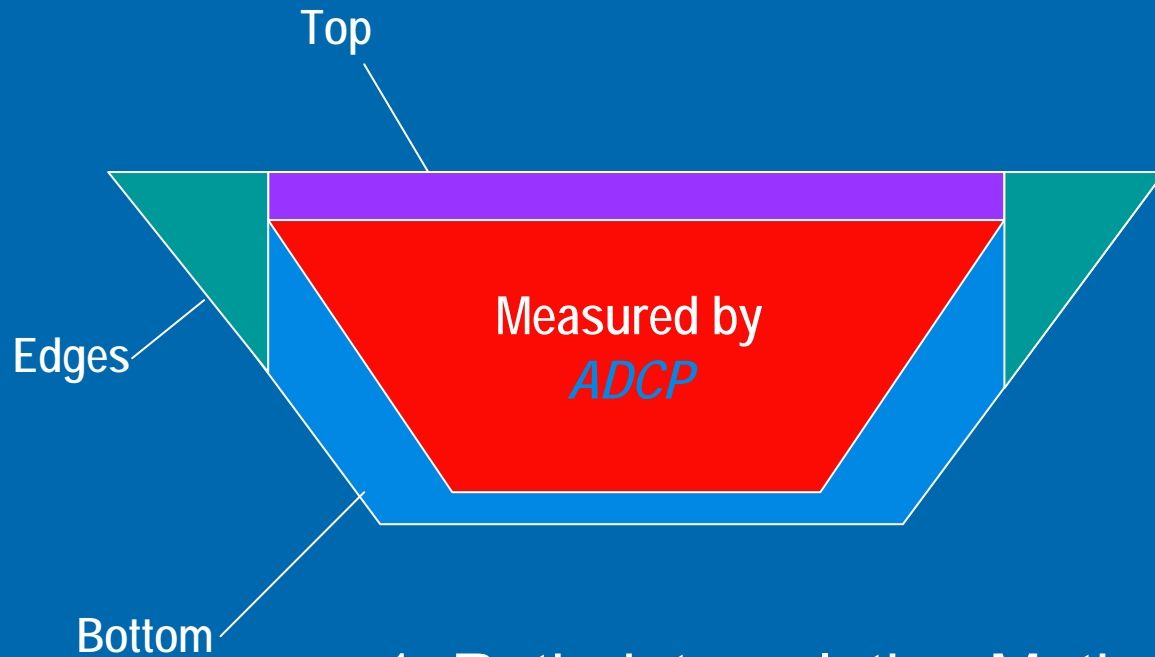
$V_{ym}$  = y-component of mean measured water-velocity vector,

$V_{bx}$  = x-component of mean vessel velocity,

$V_{by}$  = y-component of mean vessel velocity.

$dz$  = differential depth,

$t$  = elapsed time between subsections.



Estimation of  
*'unmeasured  
near bank  
sections'*

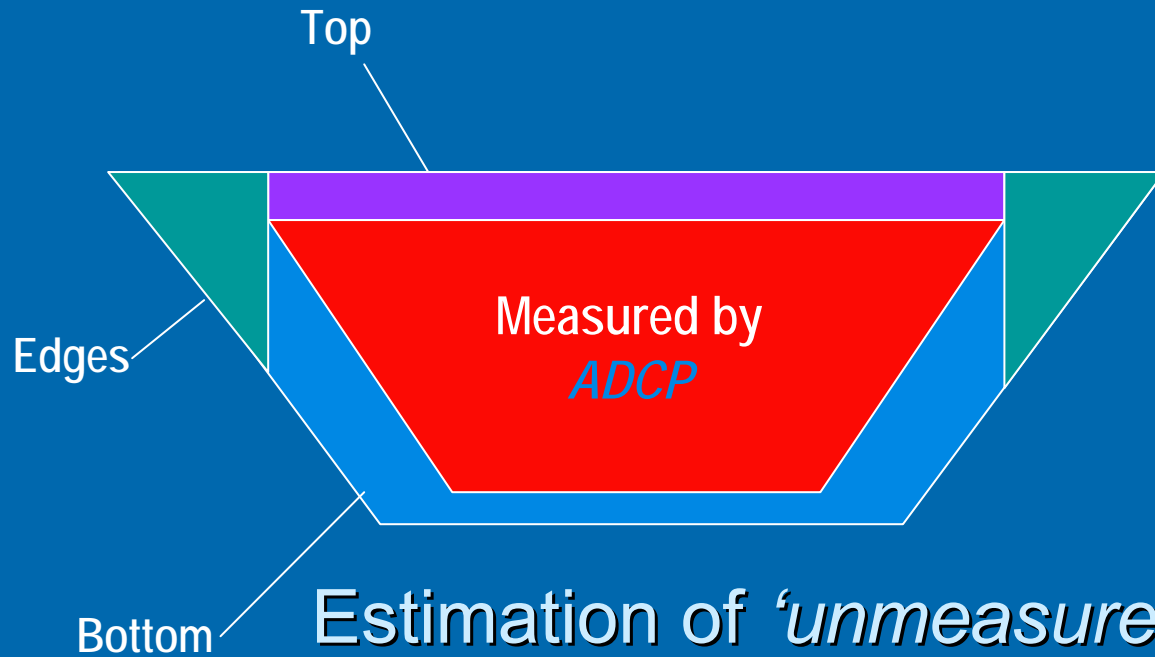
1. Ratio-interpolation Method: (Sloped-Bank)  
*Simpson and Oltmann, 1993*

$$Q_{NB} = 0.707 L \frac{d_m}{2} V_m$$

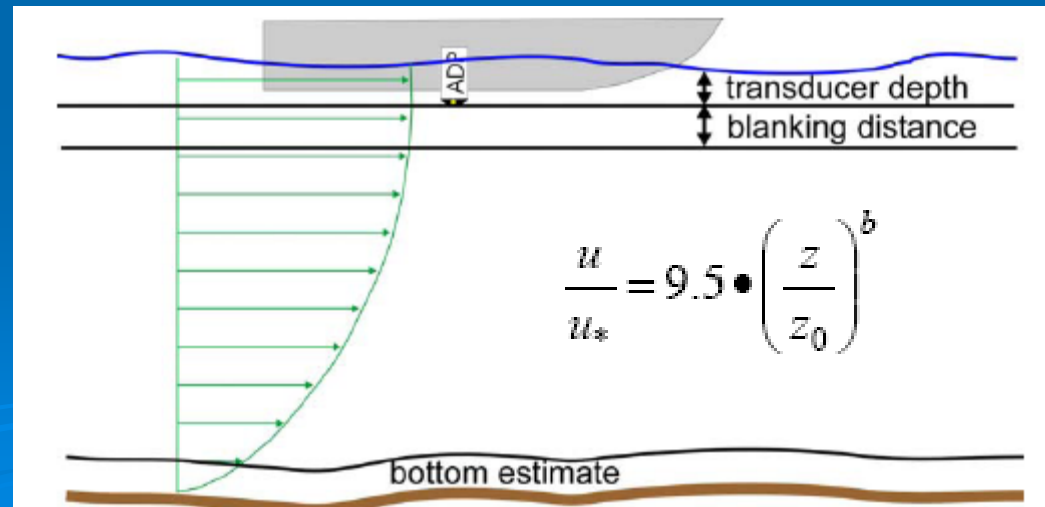
L= Distance from first/last good profile to shore,

$d_m$  = Depth of first/last good profile,

$V_m$  = Depth-averaged velocity of first/last good profile.



## Estimation of 'unmeasured top and bottom sections' by Power Law





## During flow measurements:

- Vessel should be nearly stationary at start & end.
- Avoid quick/sharp changes in vessel speed/direction.
  - Steady acceleration/deceleration
  - Maintain nearly constant speed during measurement
- **Vessel (Boat) speed should be equal to or less than water speed.**
- Taglines/tethers are helpful for maintaining very low speeds.

# During flow measurements:

Menu Bar

Tool Bar

Ship Track/Map Display

Mean profile velocity magnitude and direction 'sticks'

Discharge Summary

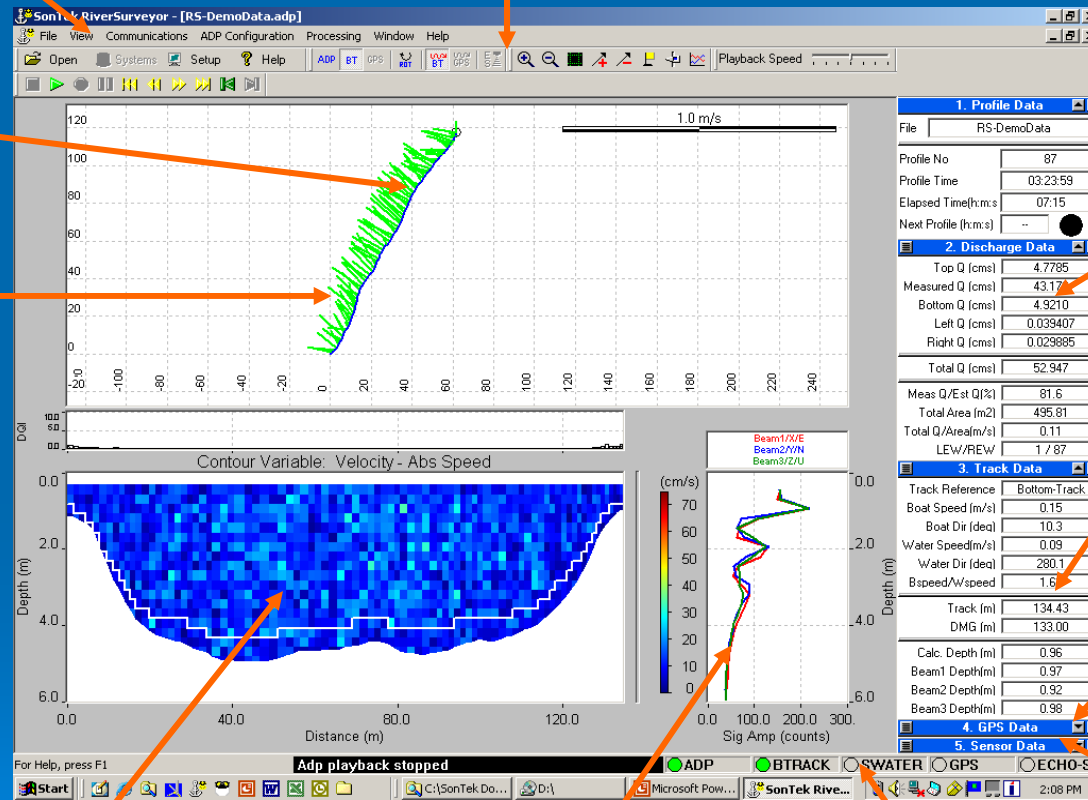
GPS Data

Sensor Display

Contour/Bottom Profile Display

Profile Graph Display

Instrument Status Displays



# Case Study 1: Acoustic measurements of flow in Tahtalı Lake via ADCP



# Case study 1: Acoustic measurements of flow in Tahtalı Lake via ADCP

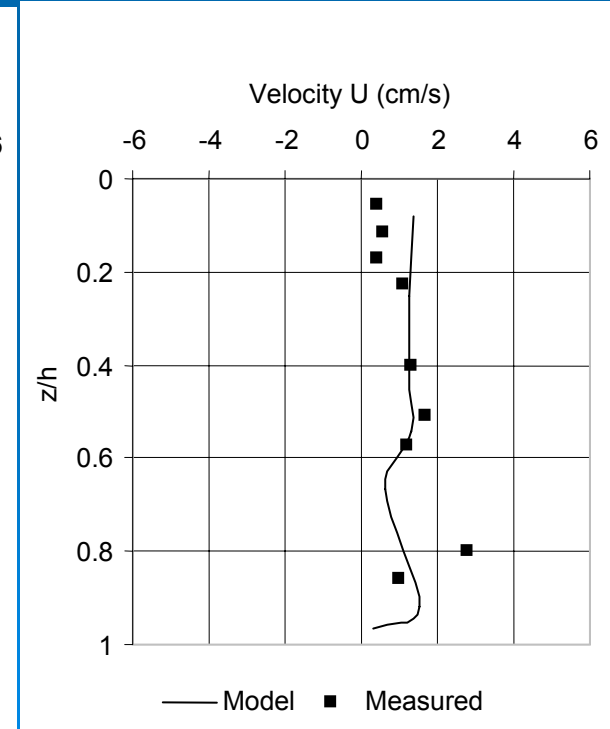
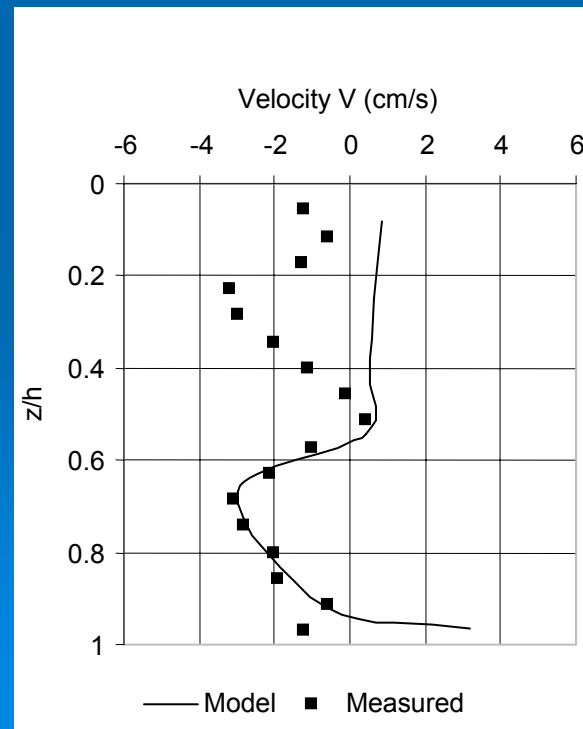
- Two projects funded by research grants from European Commission and Tubitak. Projects involved numerical modeling of hydrodynamics and sedimentation.
- Field data were collected for verification of the numerical model and prediction of processes accurately.
- EFDC numerical model requires input files which provide information about the geometry of the lake, inflows, outflows, and the meteorological data.
- The meteorological data including atmospheric pressure, air temperatures, wind speed, wind direction, humidity, solar radiation, evaporation and rain were collected at the weather station.
- The temperature profile of the water column was measured by a hand-held instrument (water quality meter).
- The discharge of the inflows was measured by Acoustic Doppler velocimeter.
- The velocity profile of the water column was measured by Acoustic Doppler current profiler which were later used to make a comparison with the model flow velocity results

# Case study 1: Acoustic measurements of flow in Tahtalı Lake via ADCP

- Velocity measurements of the water column were made using a 1.5-MHz Acoustic Doppler Current Profiler (ADCP) instrument developed by Sontek/YSI.
- The velocity vectors were measured at one location when the boat was anchored at a depth of 19 m (buoy).
- The averaging interval was set equal to profiling range (30 seconds) for continuous deployments in order to reduce the power consumption. A 1.5-MHz ADCP can operate to a profiling range (depth) of about 25 m with a minimum resolution (cell size) of 0.25 m. Cell size used during the measurements was 1 m.
- The blanking distance (0.4 m for Tahtali) of the instrument was utilized to blank out the bad data close to the transducer.

# Case study 1: Acoustic measurements of flow in Tahtalı Lake via ADCP

- Flow velocities in the water column after a 4 days simulation were compared with field observations.
- The velocity error ranged between 0.05 - 4.2 cm/s in the water column. These values are comparable with other reported values. Rueda et al. (2003) reported errors of 2 - 5 cm/s for Clear Lake; Elci and Work (2004) reported errors of 3.6 to 6 cm/s for Hartwell Lake; Jin et al. (2000) reported errors of 1.52 and 4.76 cm/s for Lake Okeechobee.



# I would recommend:

- 1) Drive the boat with a speed as low as possible
- 2) Do not change speed very drastically
- 3) Monitor both the DQI and boat/water speed BS/WS and try to get this under 1
- 4) Try to maintain low pitch and roll angles
- 5) Calibrate compass before the survey
- 6) Mount the ADCP far from the engine
- 7) Use non ferrous material for the mount otherwise it will affect the compass
- 8) Start and finish measurements in water (Check data in all times)

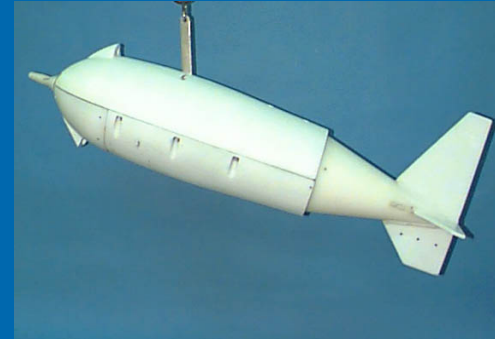
# Case Study 2: Acoustic measurements of suspended sediment concentration

- Main goal of the study:
  - To improve the methodology for predicting Suspended Sediment Concentration (SSC) in rivers using Acoustic Doppler Velocimeter (ADV).
- Existing studies: Kostaschuk et al., 2005; Alvarez et al., 2001; Gartner et al., 2002; Hosseini et al., 2006.... In these studies signal to noise ratio (SNR) and turbidity for suspended sediment concentration were related using different formulations.
- Deficiency of studies
  - Limited to single river or basin
  - Particle size effect
  - Temperature and Salinity effect



# Case Study 2: Acoustic measurements of suspended sediment concentration

- Conventional methods for collection of SSC data are labor intensive and often have large uncertainty due to spatial and temporal variability of SSC in the water column.

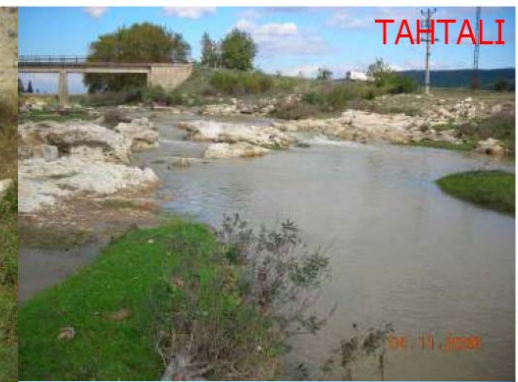
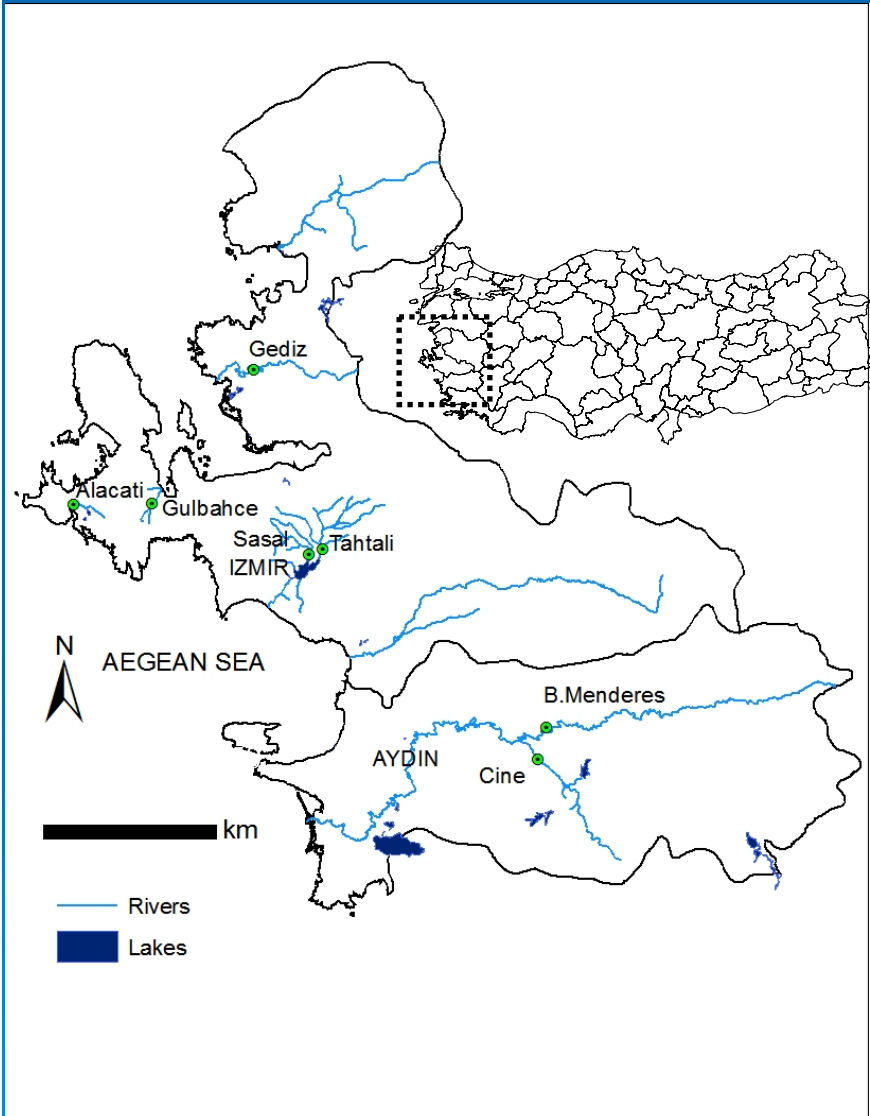


i.e. Depth-integrating samplers are designed to accumulate a water-sediment sample as the instrument is lowered to the streambed and raised to the surface at a uniform rate.

## Why use ADCPs for SSC measurements?

- simultaneous measurements and description of the whole water column and sediment suspension structure
- can use from a moving boat
- no need for additional sensor for turbidity measurements
- can measure time series of SSC profiles in the water column
- turbidity measuring instruments use optical methods which have limitations for biological fouling

# Measurement Sites



# Field Applications - Rivers



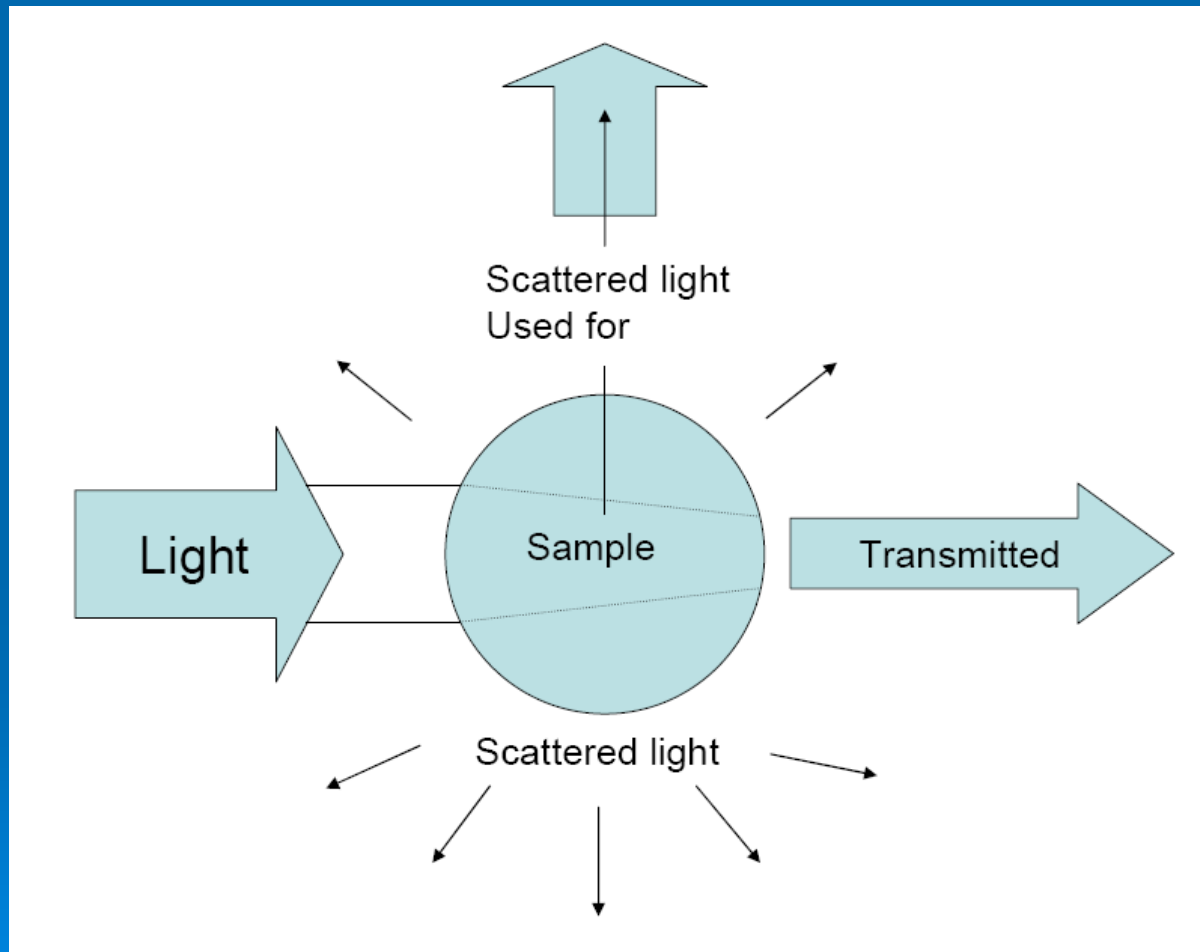
Water Quality  
Meter



Acoustic Doppler  
Velocimeter (ADV)  
Flowtracker  
(10,000 kHz)



# Turbidity measurements by optical method



# Acoustic measurements of SSC

## Methodology

Simultaneous measurements were made with ADV and WQC.

- The **Sonar equation** is used to determine signal strength.

$$EL = SL + 10 \times \log(PL) - 20 \times \log(R) - 2 \times \alpha \times R + Sv + RS$$

Where;

$EL$  = "Echo Level" is the signal strength as measured by the instrument.

$SL$  = "Source Level" is a measure of transmitted acoustic power

$PL$  = "Pulse Length" is the length of the acoustic pulse.

$R$  = Range between the transducer and the measurement volume

$\alpha$  = Sound absorption coefficient (dB/meter)

$Sv$  = Volume scattering strength (dB)

$RS$  = "Receive Sensitivity" expresses the relationship between pressure at transducer face and measured signal strength

# Acoustic measurements of SSC

## Methodology

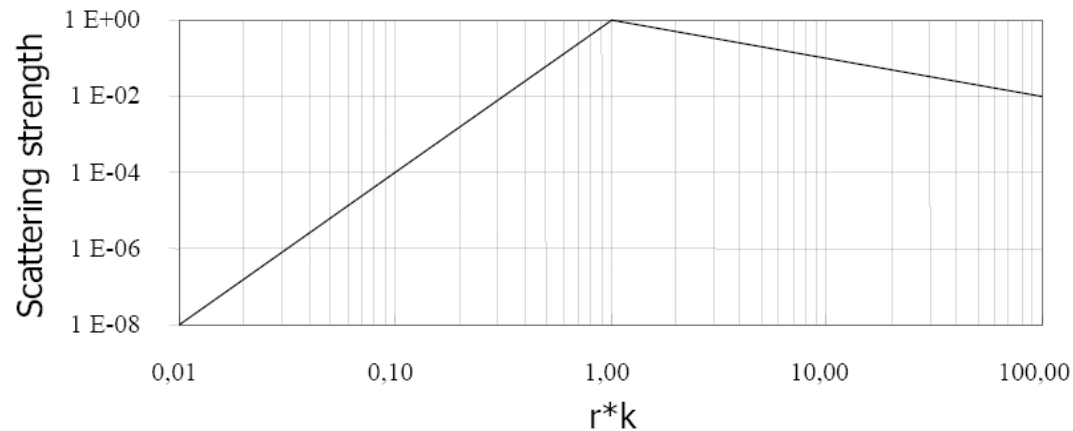
- The signal strength decreases with the range due to;
  - Geometric spreading
  - Absorption
- The absorption coefficient of water is a function of
  - Frequency
  - Salinity
  - Temperature
  - Pressure
- Absorption coefficients ( $\alpha$ ) were estimated by the formula defined by Shulkin and Marsh (1962):

$$\alpha = \left( \frac{SAf_t f^2}{f_T^2 + f^2} + \frac{3.38 \times 10^{-6} f^2}{21.9 \times 10^{6 - [1520 / T + 273]}} \right) (1 - 6.54 \times 10^{-4} P)$$

# Acoustic measurements of SSC

## Methodology

- Soil samples were collected from the rivers
  - Sieve analysis (in ASTM standard)
  - Hydrometer analysis (in ASTM standard)
- Acoustic instruments have different sensitivities to particle size. For our instrument (10,000 kHz ADV);
  - Best sensitivity is expected for particle radius close to **0.025 mm**
  - Minimum detectable particle radius is **0.001 mm**



# The Multivariate Data Analysis

Since both dimensionless mean sediment diameter ( $\frac{d_{50}}{d_{50b}}$ ), and coefficient of gradation ( $C_g$ ), are soil properties, these two parameters were combined by multiplication and PLS analysis was conducted using a data matrix of four variables (SSC, SNR,  $\frac{\alpha}{\alpha_c}$ ,  $\frac{d_{50}}{d_{50b}} \times C_g$ ).

$$\alpha = 8.687 \times \frac{3.38 \times 10^{-6} f^2}{21.9 \times 10^{6 - [1520/T + 273]}}$$

$\alpha$  is the absorption coefficient and  $\alpha_c$  for the calibration temperature (4 °C)

A new PLS model was utilized based on these four parameters. The following equation gave the relationship between these parameters:

$$SSC = -13.8 + 0.8 \times SNR + 21.04 \times \frac{\alpha}{\alpha_c} + 4.52 \frac{d_{50}}{d_{50b}} \times C_g$$



# The Multivariate Data Analysis

- Simca-P 10.5 estimates the predictive ability of the model defined by predicted residual sum of squares ( $Q^2$ ) by cross-validation. The data are divided into 7 parts and a model is built on  $(6/7)^{\text{th}}$  of the data, where the omitted data are predicted from the new model. This is repeated with each  $(1/7)^{\text{th}}$  of the data until all the data have been predicted (Umetrics 2003). The predicted data are then compared with the original data and the sum of squared errors calculated for the whole dataset.  $Q^2$  was calculated as 0.90 for the model. The computed MAE [Mean Absolute Error] and MRE [Mean Relative Error] for Equation were 1.88 mg/L and 10%, respectively.

## Case Study 3: Utilizing acoustic methods to predict reservoir sedimentation

- Surveying of Tahtali reservoir via dual frequency (28/200 kHz) echo-sounder system to determine the current bathymetry
- Estimation of sediment thickness from the difference of depths measured by the dual frequency sounder along surveyed transects.
- Comparison of the results to the modeled sedimentation thicknesses and to preliminary estimates of watershed sediment yield estimated by USLE

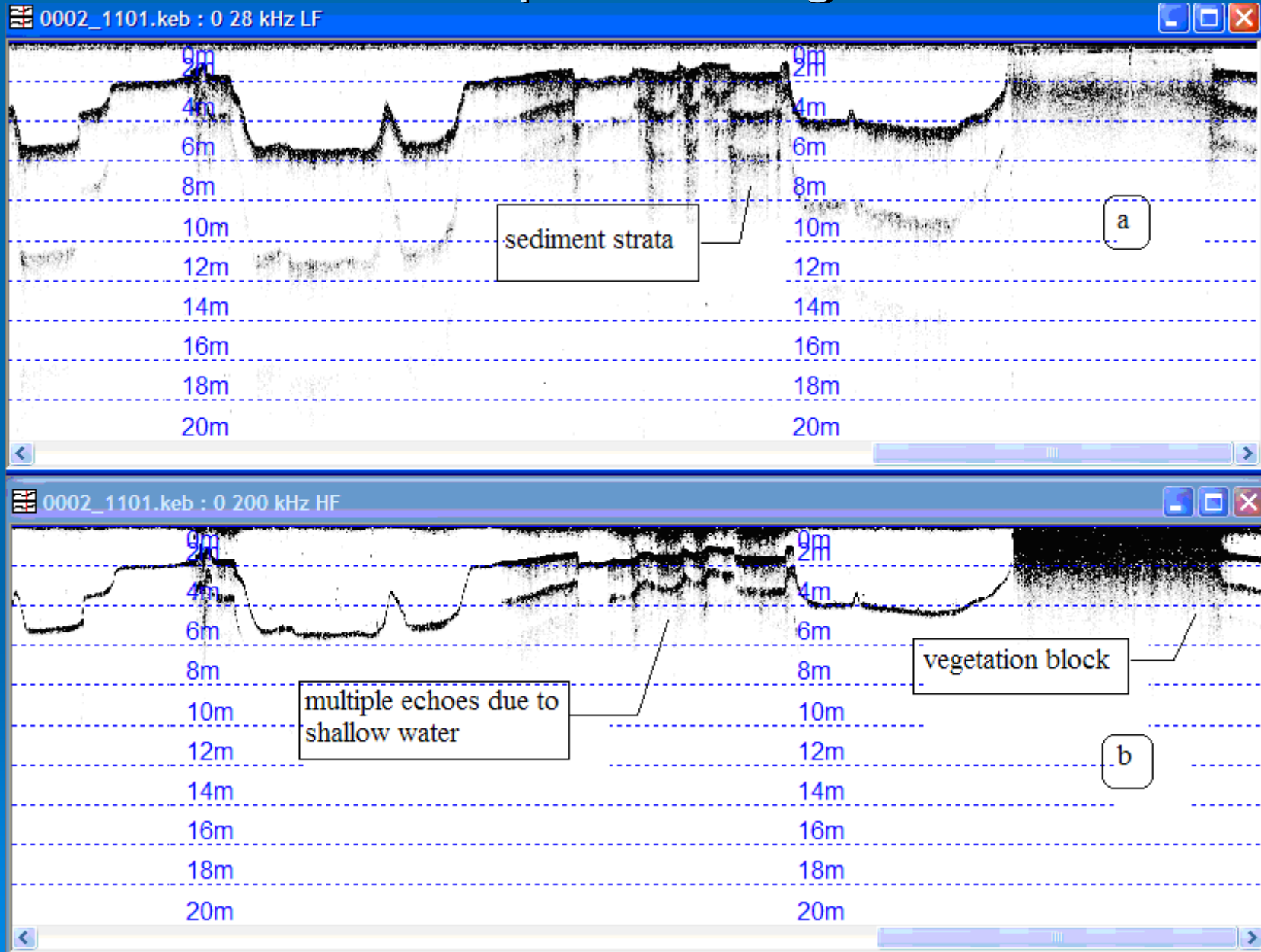
# Case Study 3: Utilizing acoustic methods to predict reservoir sedimentation

- The principle of echo sounder is composed of transmitting ping and listening to the return of the echo. The depth of the water is estimated by measuring the time for the transmitted ultrasound pulse to return.
- The high frequency (200 kHz) sound wave tracks the top of the sediment, where the low frequency (28 kHz) wave penetrates through the sediment to a more solid bottom. The advantage of using a dual frequency echo sounder is that sediment thickness can be estimated from the different echoes generated at the interface between water (low impedance) and sediment (high impedance) layers.

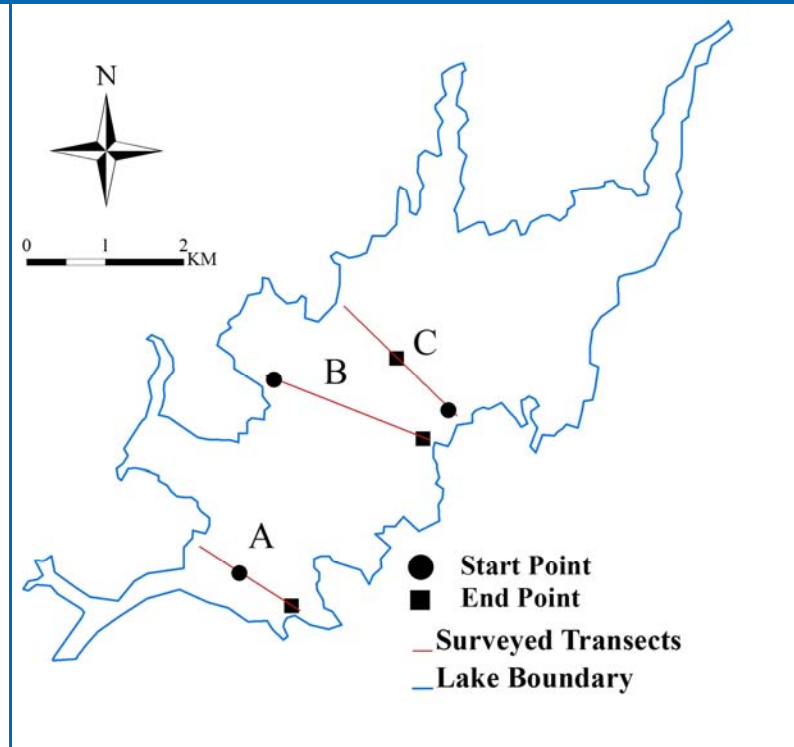
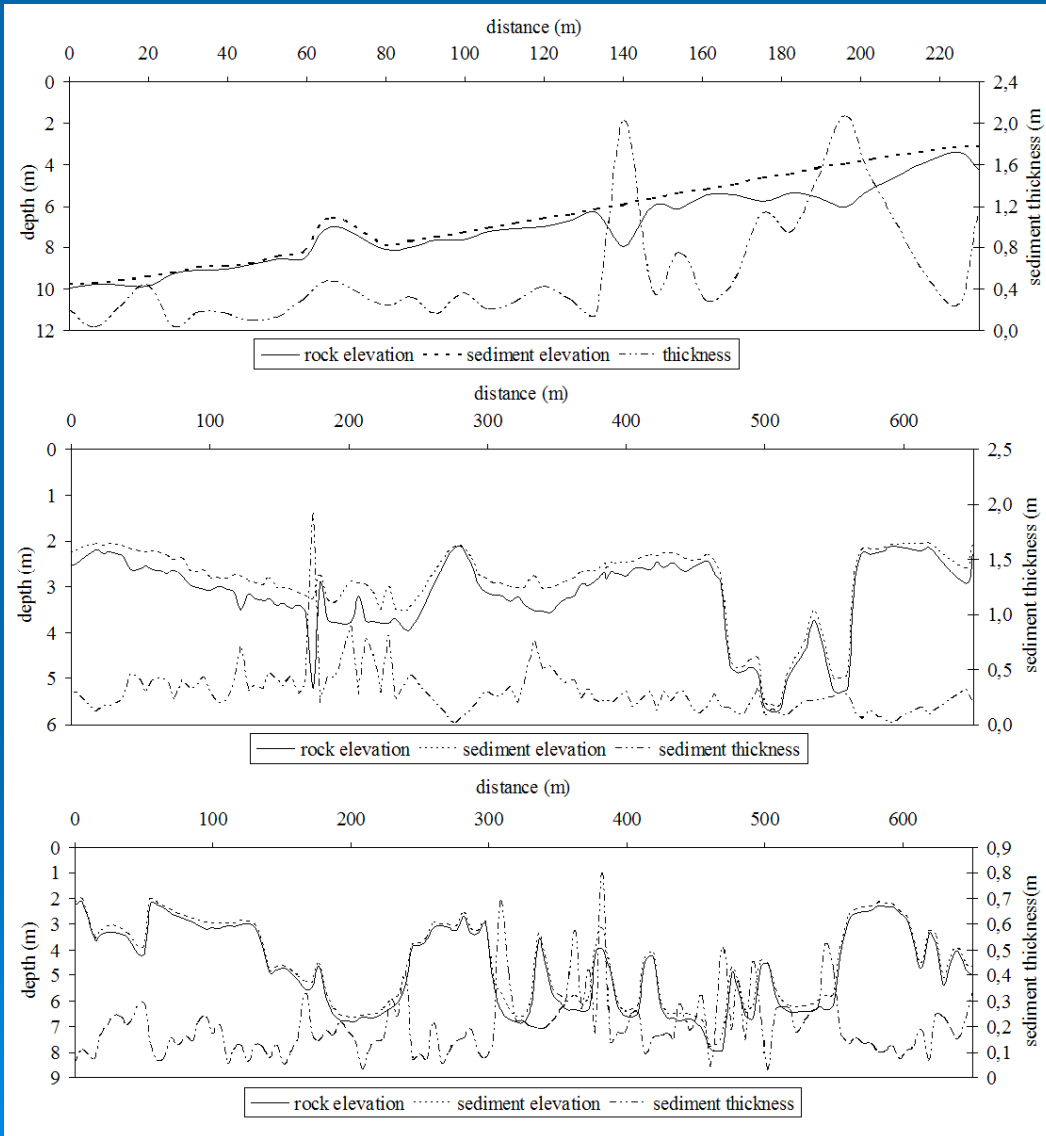


320 B/P dual frequency echo sounding system (by Knudsen Engineering)

# Sample readings



# Surveyed transects



# Prediction of erosion by USLE

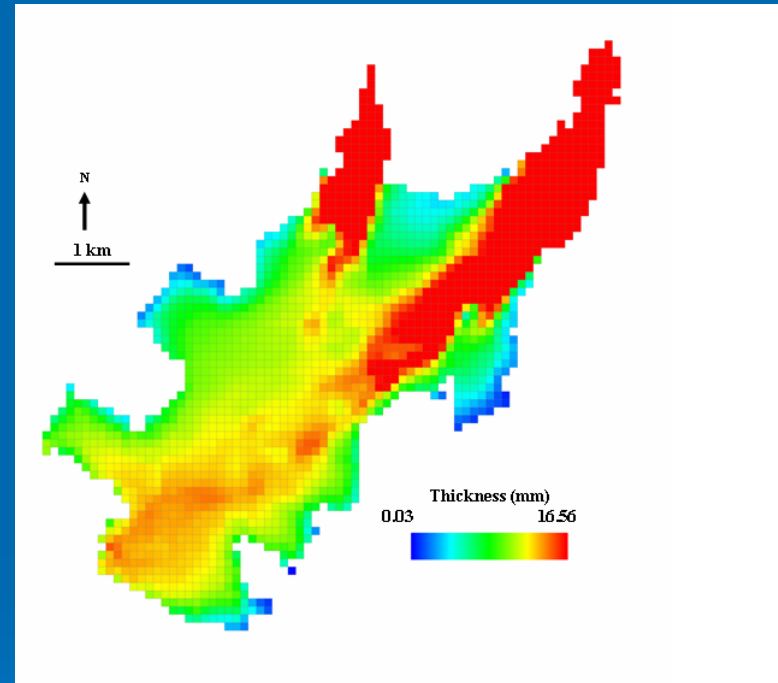
- For quantification of soil loss within the watershed, soil and topographic maps of the basin were constructed into a vector type spatial database using the GIS.
- The average annual soil erosion rate was calculated using USLE

$$A = RKLSCP$$

- where;  $A$  is the average annual soil loss in t/ha-year;  $R$  is the rainfall erosivity factor in MJ-mm/h-ha-year representing the annual sum of the products between the energy of the erosive rainfalls in MJ/ha and their intensity in mm/h;  $K$  is the soil erodibility factor in t-ha-h/ha-MJ-mm;  $L$  is the slope length factor (unitless);  $S$  is the slope steepness factor (unitless);  $C$  is the cropping management factor (unitless);  $P$  is the supporting practice factor (unitless).

# Sedimentation Results

- For the prediction of sedimentation patterns lake wide, the EFDC model was applied to the lake. Soil loss predicted by USLE was utilized as input to the hydrodynamic and sediment transport model since long term measurements of sediment concentrations were not available.
- The modeling results were also compared to survey results where a dual frequency (28/200 kHz) echosounder system, and global positioning system navigation (GPS) were utilized for surveying of the lake.
- Sediment thickness modeled by the numerical model was 23 cm in average for the surveyed area and this was comparable with the survey results which gave an average thickness of 25 cm.



# Hydrodynamics of Lakes and Reservoirs

General processes: focus on  
sediment transport

ERASMUS LECTURES PREPARED  
FOR LUND UNIVERSITY

**Assoc.Prof.Dr.ŞEBNEM ELÇİ**

IZMIR INSTITUTE OF TECHNOLOGY  
CIVIL ENGINEERING DEPT.




# Why study sediment transport?

- Proper management of water resources requires knowledge of sediment load and yield.
- The planning of hydraulic structures such as dams, canals, etc. is practically impossible without sediment data.
- Sediment deposition in stream or river channels can cause flooding.
- **\*\*\* Physical, chemical and biological sediment damage in North America has been estimated to be up to \$16 billions annually .**



# Sediment transport studies focus mainly on:

- (1) **Sediment Yield:** e.g. impacts on receiving waters (reservoir filling; water quality; mining)
- As rivers enter reservoirs, the flow depth increases and flow velocity decrease  $Q=VA$  . This reduces sediment transport capacity and causes settling. Sediments depositing in the lake causes filling of the reservoir and changes the life expectancy of reservoir.
  - Heavy metals have affinity to attach to cohesive sediments of fine sediments. They can be transported to long distances in a lake before they deposit.
  - Mining operations may introduce volumes of sediment directly into natural streams. Mine dumps continue to erode by rainfall for many years after mining operations have ceased.
- 

# Sediment transport studies focus mainly on:

**(2) Channel change:** bed aggradation/degradation, bank erosion (navigation, flood levels, bridge and bank protection)

- Human activities influence erosion. Erodibility of materials is enhanced by disturbances such as cutting and burning of trees.
- Bridges on streams can experience scour problems and cause major bridge failures during floods.

In general, channel change is a function of water and sediment supply & the basic sediment transport questions are:

- How much sediment can the channel transport with the available water?
- Is this transport rate greater or smaller than the rate at which sediment is being supplied to a reach?

# Initiation of particle motion

- Main question is the critical condition for beginning of motion of particles
- A critical condition is a function of;  
 $f(V, h, B, S, g, k, \rho, \gamma, d_s, SF, \rho_s, \zeta)$

Flow charac.	Fluid prop.	Sediment prop.
V, velocity	$\rho$ , density	$d_s$ , size
h, depth	$\gamma$ , viscosity	SF, shape factor
B, channel width		$\rho_s$ , density
S, slope		$\zeta$ , size distribution
g, gravity		
k, bed roughness		

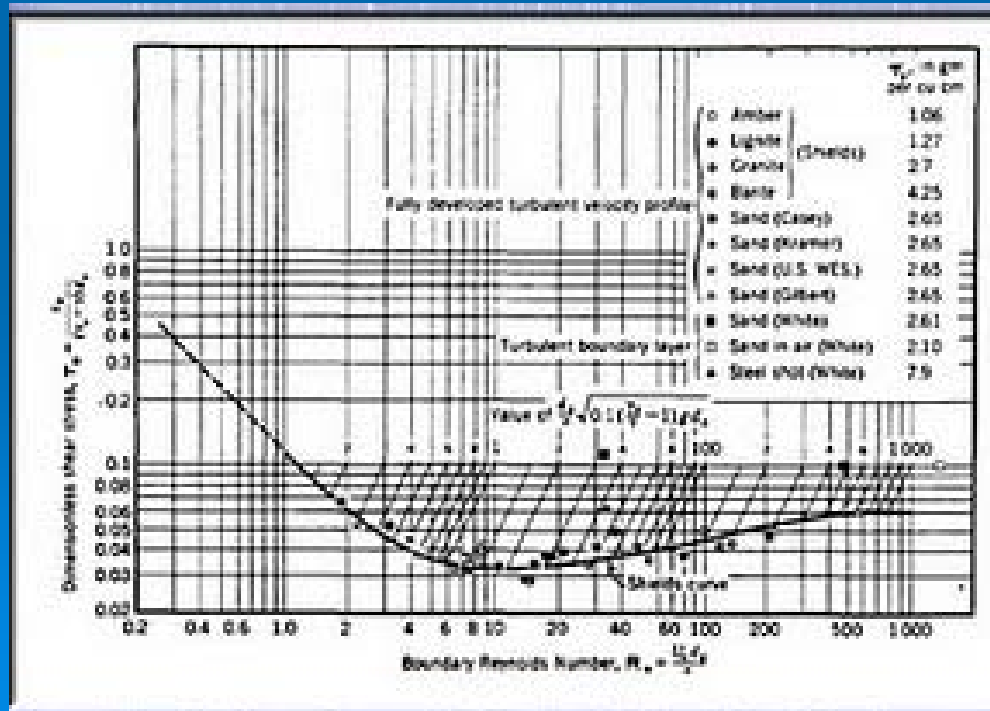
# Initiation of particle motion

From dimensional analysis:

- Shields (1936) gave the most known formula for uniform flow where he gave a relation between dimensionless shear stress and particle Reynolds number. Shear stress and critical velocity are dependent values

Re < 1 hydraulically smooth Re > 600 rough and

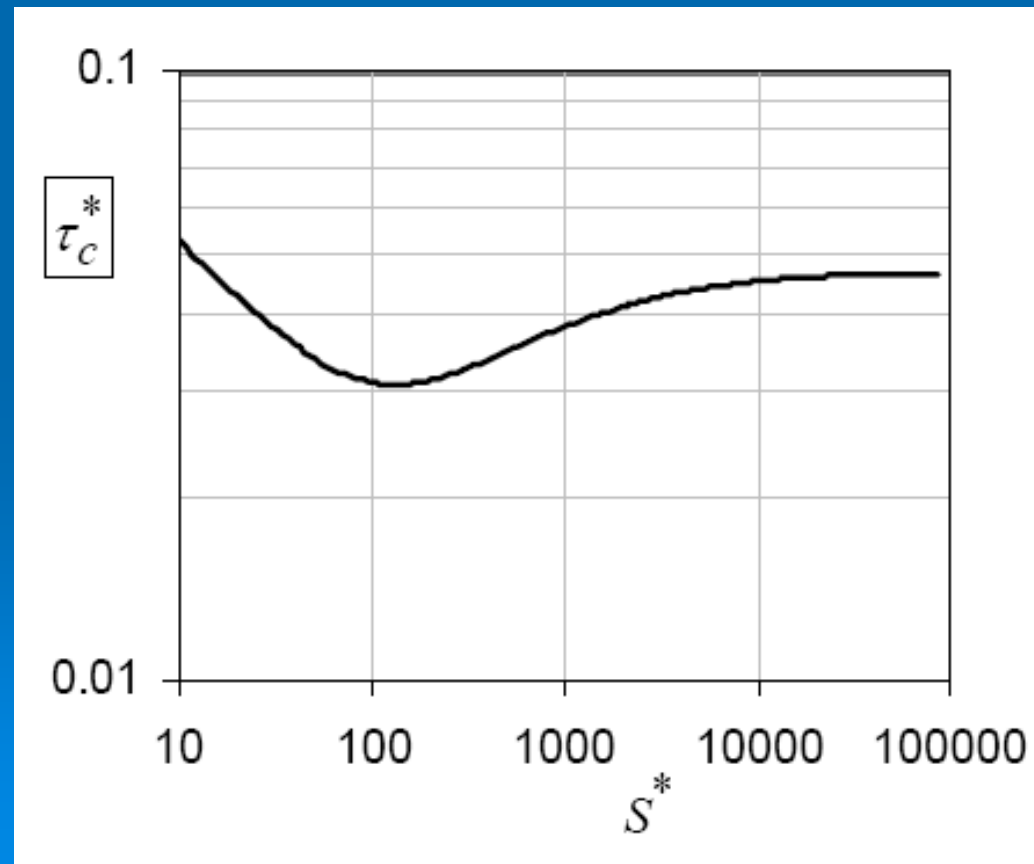
$$\frac{\tau_c}{(\gamma_s - \gamma)d_s} = 0.06$$



$$\psi_c = \frac{\tau_c}{(\rho_s - \rho_w)gd} = \frac{u_{*c}^2}{\Delta gd} = f(Re_*) = f\left(\frac{u_{*c}d}{\nu}\right)$$

The trend of the Shields' curve can be formulated as:

$$\tau_c^* = 0.105(S^*)^{-0.3} + 0.045 \exp\left[-35(S^*)^{-0.59}\right]$$



# Mechanisms of Sediment Transport

- Sediments either are eroded from basin by water (sheet erosion) and transported to the stream as **wash load**
- Or eroded by streamflow from the stream bed and transported as **bed load**.



Suspended load (lower channel) and bedload (clear upper channel) confluence, Costa Rica, *Photograph by Richard Kesel*

## Bed load vs. Wash load

- Bed load is a function of *flow characteristics*
- Wash load is a function of *hydrological characteristics* of a drainage basin (such as size, soil properties, topography, intensity/duration of precipitation, vegetation, winds, surface flow)
- Empirical approach for classification:
- $D_5$  or  $D_{10}$  is used as a limit
  - if sediment  $< D_5$  : wash load
  - if sediment  $> D_5$  : bed load
- In general 5-20 % of total load is transported as bed load.
- Bed load transport rate determines bed stability whereas wash load transport rate determines rate of reservoir deposition



## Particles move in 3 different forms:

- Bed load: When the critical conditions are exceeded particles will start moving by sliding/rolling
- Saltation: Particle is detached and reattached by gravity and fluid resistance (neglected)
- Suspension: Flows at high velocities are turbulent and have eddies. If a particle jumping from bed enters such an eddy, it is carried away in suspension
  - Suspension takes energy from turbulent flow, suspended load reduces turbulent intensity

# Initiation of suspension from bed load:

➤ **Kressler (1964):**

$$\frac{V^2}{gd} = 360$$

For 0.3 mm sediment size, critical flow velocity for suspension is 1 m/s

➤ **Bagnold (1966):**

$$\frac{w}{u_*} = 1.25$$

related settling velocity to shear velocity, no particles remain in suspension unless upward velocity of turbulent eddies exceeds settling velocity

➤ **Van Rijn (1984):** for

$$1 < d_* < 10$$

$$\frac{u_*}{w} = \frac{4}{d_*}$$

for

$$d_* > 10$$

$$\frac{u_*}{w} = 0.4$$

➤ **Sümer (1986) :**

$$\text{Re}_* = \frac{u_* d}{\gamma} < 70$$

$$\text{Re}_* = \frac{u_* d}{\gamma} > 70$$

$$\tau_* = \frac{17}{\text{Re}_*}$$

$$\tau_* = 0.27$$

$$\tau_* = \frac{u_*^2}{\frac{\rho_s - \rho_w}{\rho_w} gd}$$

$$d_* = \left( \frac{\frac{\rho_s - \rho_w}{\rho_w} g}{\gamma^2} \right)^{1/3}$$

# Modes of transport / Bed load

- Bed load is concerned with two phase (solid+liquid) flow near river bed.
- Several eqns are developed for steady uniform equations, where constants are determined experimentally.
- Difficult to measure bed load since measuring devices disturb bed.
- Different approaches are available (mainly using force, and power). Bedload formula approaches include:
  - Shear stress,
  - Energy slope,
  - Discharge,
  - Velocity,
  - Bed form,
  - Probabilistic,
  - Stochastic,
  - Regression, and
  - Equal mobility approaches.

# Modes of transport / Bed load

- When the flow conditions exceed the criteria for incipient motion, sediment particles on the streambed start to move. The transport of bed particles in a stream is a function of the fluid forces per unit area: the tractive force or shear stress, acting on the streambed.

- Under steady, uniform flow conditions, the shear stress is

$$\tau = \gamma DS$$

- The gravitational force resisting particle entrainment, is proportional to:

$$f_g \propto (\gamma_s - \gamma) d$$

- The Shields relation (Shields 1936) with modifications by Graf (1971) developed relations associated with initiation of particle movement using the ratio of the fluid forces to the gravitational force, proportional to the dimensionless quantity called the critical dimensionless shear stress,  $\tau_c^*$ , where:

$$\tau_c^* \propto \frac{DS}{(\gamma_s - \gamma)d}$$



# Modes of transport / Bed load

- The dimensionless bed-material transport rate per unit width of streambed,  $Q_B^*$  is:

$$Q_B^* = \frac{Q_s}{[(\gamma_s - \gamma)gd]^{1/2} d}$$

where:

$g$  is gravity, and

$Q_s$  is the volumetric transport rate per unit width of streambed determined from bedload samples.

The empirical function developed by Parker (1979) is

$$Q_B^* = \frac{11.2 (\tau^* - \tau_c^*)^{4.5}}{(\tau_c^*)^3}$$

where:

$\tau_c^*$  is the threshold value of  $\tau$  required to initiate particle motion.

# Modes of transport / Suspended Load

- When particles leave the bed, they can move for a long distance without settling down, since their settling velocities are balanced by upward vertical component of turbulent velocity .
- To determine rate of suspended load transport we must know concentration distribution

$$C = f(C_a, a, y, h, u_*, w)$$

Equating the rates of transport in the upward and downward directions, and assuming that mass transfer coef. is proportional to coef. of momentum transfer:

$$\tau_l = \rho \varepsilon_m \frac{du}{dy} = \rho l^2 \left( \frac{du}{dy} \right)^2$$

(Rising by diffusion)

$$-\varepsilon_s \times \frac{dC}{dy}$$



$$w \times C$$

(Settling by gravity)

# Modes of transport / Suspended Load

- Assuming logarithmic velocity distribution, where k is Karman's constant (=0.4):

$$\frac{du}{dy} = \frac{U_*}{ky}$$

- Shear stress varies linearly in an open channel flow of depth h,

$$\tau_l = \tau_0 \left(1 - \frac{y}{h}\right) = \rho U_*^2 \left(1 - \frac{y}{h}\right)$$

- Combining these expressions, assuming that mass transfer coeff. is proportional to coef. of momentum transfer:

$$w \times c + U_* \times k \times y \times \left(1 - \frac{y}{h}\right) \times \frac{dC}{dy} = 0$$

- Integrating (Rouse equation -1937):

$$\frac{C}{C_a} = \left( \frac{h-y}{y} \times \frac{a}{h-a} \right)^\alpha$$

$$\alpha = \frac{w}{\beta k u_*}$$

- Where  $C_a$  is the reference concentration at  $y=a$

# Case Study: Experimental and Numerical Investigation of Bedload Transport Under Unsteady Flows

- The project is funded by research grants from Tubitak
- The dynamic behavior of bedload sediment transport ***under unsteady flow conditions*** is experimentally and numerically investigated. A series of experiments are conducted in a rectangular flume (18 m length, 0.80 m width) with various triangular and trapezoidal shaped hydrographs.
- The experimental data were also qualitatively investigated employing the unsteady flow parameter and total flow work index.
- One-dimensional numerical model, which employs the governing equations for the conservation of mass for water and sediment and the momentum, was also developed to simulate the experimental results.



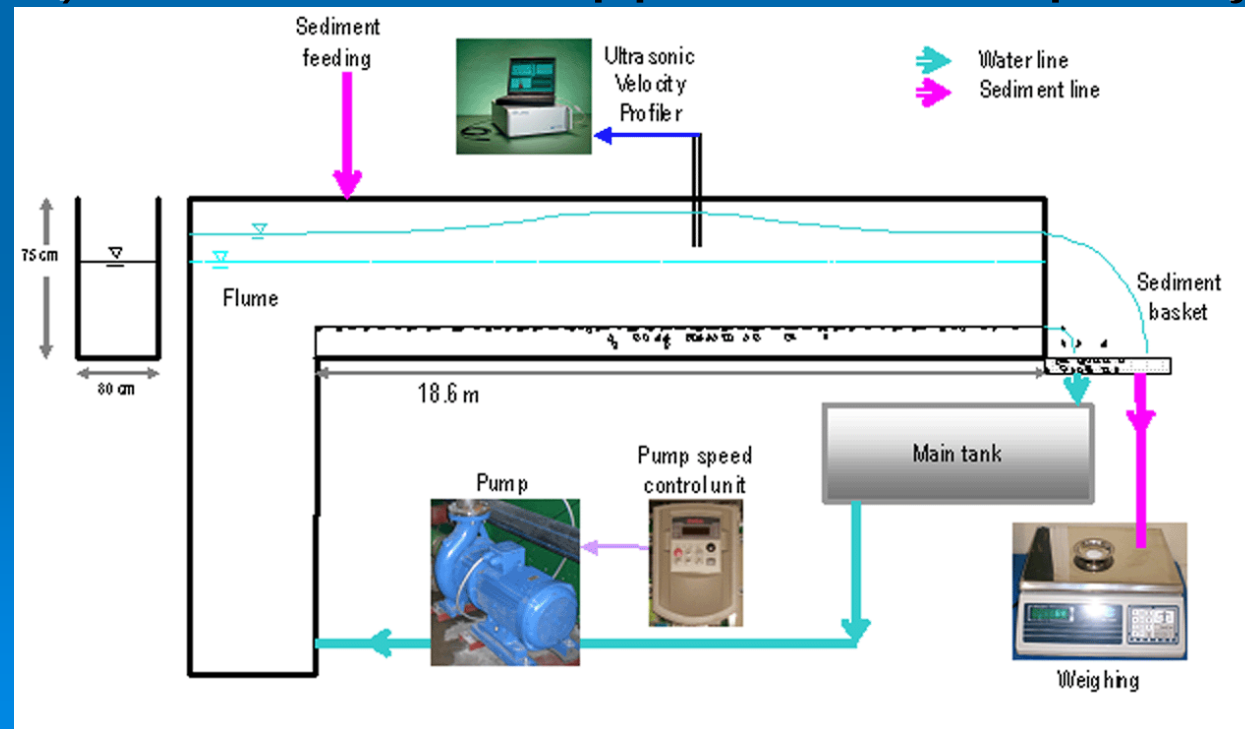
# Case Study: Experimental Setup

- Experiments are carried out in a recirculating rectangular flume, with a width of 80 cm and length of 18.6 m.
- The transparent sides of the channel are 75 cm high.
- The slope of the flume is adjustable and set to 0.005.
- The volume of the water supply reservoir is 27 m<sup>3</sup>.
- The steel channel's rigid bed is overlaid with 8 cm thick, uniform small gravel with  $d = 4.8$  mm.
- The uniformity coefficient of the soil is  $Cu = 2.2$  implying that the sample is uniform.



# Case Study: Experimental Setup

- The flow rate in the flume is controlled and preset by a speed control unit attached to pump system with a maximum capacity of 100 l/s. The velocities are measured by 2 MHz UVP (Ultrasonic Velocity Profiler) which uses Doppler shift frequency.



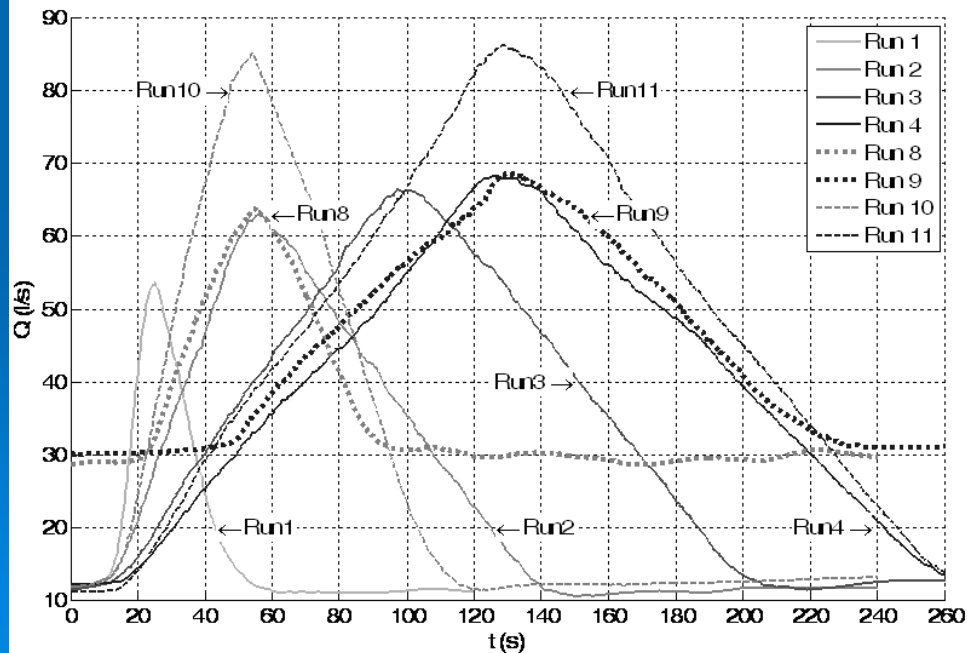
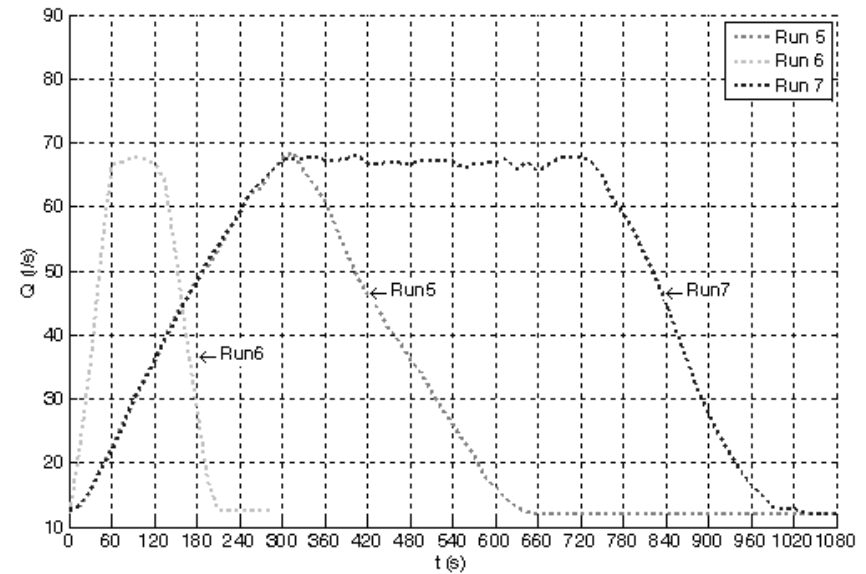
## Case Study: Experimental Setup

- The bed elevations were obtained by 4 MHz UVP with a transducer vertically oriented.
- During the steady flow experiments, the threshold value of shear stress for the initiation of sediment motion was obtained.
- At the downstream of the flume, the bed load is collected every 15 seconds using baskets composed of very fine meshed nets. Upon drying, the sediments are weighed to estimate the variation of total bed load with time.



# Case Study: Experiments

- A series of triangular and trapezoidal shaped hydrographs were simulated.



## Case Study: Experiment Results

- Table 1 Parameters estimated from various hydrographs. [ $t_r$  : time to peak rate of hydrograph,  $t_d$  : duration of hydrograph,  $t_{sp}$  : time to peak rate of sedimentograph,  $t_{lag}$  : difference between peak times ( $t_{sp} - t_r$ ),  $y_0$  : water depth at base flow,  $y_p$  : water depth at peak flow,  $u^*_0$  : shear velocity at base flow,  $u^*_p$  : shear velocity at peak flow,  $W_R$  : total bed load collected during the rising stage,  $W_F$  : total bed load collected during the recession stage,  $u_0$  : velocity of the base flow hydrograph,  $u_p$  : velocity of the peak flow hydrograph]

Run no	$t_r$	$t_d$	$t_{sp}$	$t_{lag}/t_r$	$y_0$	$y_p$	$u^*_0$	$u^*_p$	$W_R$	$W_F$	$W_R / W_F$	$W_R / W_t$
1	14	67	22.5	0.61	0.04	0.09	0.04	0.07	400	427	0.94	0.48
2	46	150	67.5	0.47	0.04	0.10	0.04	0.07	1256	1611	0.78	0.44
3	90	208	97.5	0.08	0.04	0.10	0.04	0.07	1737	2213	0.79	0.44
4	119	267	127.5	0.07	0.04	0.10	0.04	0.07	2499	2755	0.91	0.48
5	300	645	322.5	0.08	0.04	0.11	0.04	0.07	7164	5098	<b>1.41</b>	0.58
6*	60	210	82.5	0.38	0.04	0.11	0.04	0.07	2262	1869	<b>1.21</b>	0.55
7*	300	990	337.5	0.13	0.04	0.11	0.04	0.07	7180	4356	<b>1.65</b>	0.62
8	34	99	38.5	0.13	0.07	0.10	0.06	0.07	922	1093	0.84	0.46
9	82	187	89.5	0.09	0.07	0.10	0.06	0.07	1887	2452	0.77	0.43
10	44	136	52.5	0.19	0.04	0.12	0.04	0.08	1877	2411	0.78	0.44
11	118	270	127.5	0.08	0.04	0.12	0.04	0.08	4755	4843	0.98	0.50

# Case Study: Experiment Results

- Vol : total volume of water under the hydrograph, P : unsteady flow parameter, P<sub>mod</sub> : modified unsteady flow parameter, P<sub>gt</sub> : proposed unsteady flow parameter, W<sub>k</sub> : total flow work, W<sub>t</sub> : total bed load, W<sub>t</sub>\* : dimensionless total bed load]

Run no	$u_0$	$u_p$	Vol	P	P <sub>mod</sub>	P <sub>gt</sub>	W <sub>k</sub>	W <sub>t</sub>	W <sub>t</sub> *
1	0.38	0.77	0.26	0.016	0.007	0.0021	0.4	0.8	15.4
2	0.38	0.78	1.41	0.009	0.004	0.0041	1.9	2.9	59.0
3	0.38	0.80	2.50	0.007	0.002	0.0045	3.4	4.0	80.9
4	0.38	0.83	3.38	0.005	0.001	0.0046	4.7	5.3	107.5
5	0.38	0.79	8.50	0.002	0.001	0.0049	11.7	15.3	313.6
6*	0.38	0.79	4.16	0.007	0.003	0.0043	5.7	8.0	163.8
7*	0.38	0.79	23.47	0.002	0.001	0.0049	32.3	41.9	857.2
8	0.57	0.79	1.27	0.006	0.001	0.0043	1.7	2.0	40.9
9	0.57	0.83	3.73	0.003	0.000	0.0047	5.1	4.3	88.9
10	0.38	0.90	2.20	0.013	0.006	0.0038	3.0	4.3	87.8
11	0.38	0.90	5.21	0.007	0.002	0.0046	7.2	9.6	196.5

## Case Study: Unsteadiness Parameter and Total Flow Work

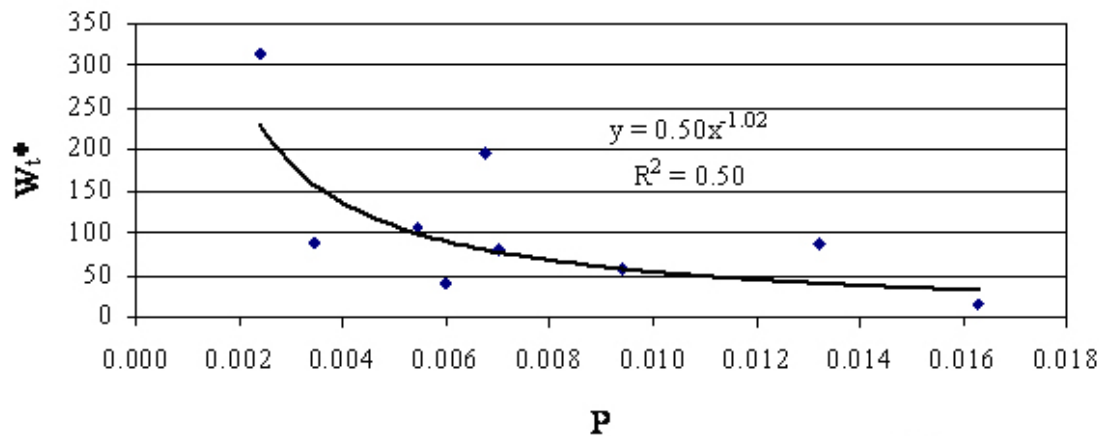
- Although many empirical sediment transport formulations exist in the literature, application of these relationships to unsteady phenomena might give erroneous results due to accelerations in the unsteadiness character of the problem.
- In the literature, the unsteadiness character of the flow is investigated through the unsteady flow parameter and total flow work (Graf and Suzka 1985, Yen and Lee 1995, Song and Graf 1997, and Lee et al. 2004).

$$P = \frac{h_p - h_0}{t_d u_{*0}} \quad W_k = \frac{u_{*0}^2 V_{ol}}{g h_0^3 B}$$

where  $B$  is channel width,  $V_{ol}$  is total volume of water under the hydrograph (excluding the baseflow),  $u_{*0}$  is the shear velocity of the baseflow at the upstream end calculated as a function of slope and hydraulic radius,  $h_0$  is the initial flow depth (baseflow) at the upstream end,  $h_p$  is the flow depth at the peak of the hydrograph at the upstream end and  $t_d$  is the duration of the hydrograph.

# Case Study: Unsteadiness Parameter and Total Flow Work

- De Sutter et al (2001) discussed the effectiveness of unsteadiness parameter with respect to the duration of both the rising and descending limbs. They stated that only the duration of the rising limb should be considered in the unsteadiness of the hydrograph and proposed the following parameter instead:

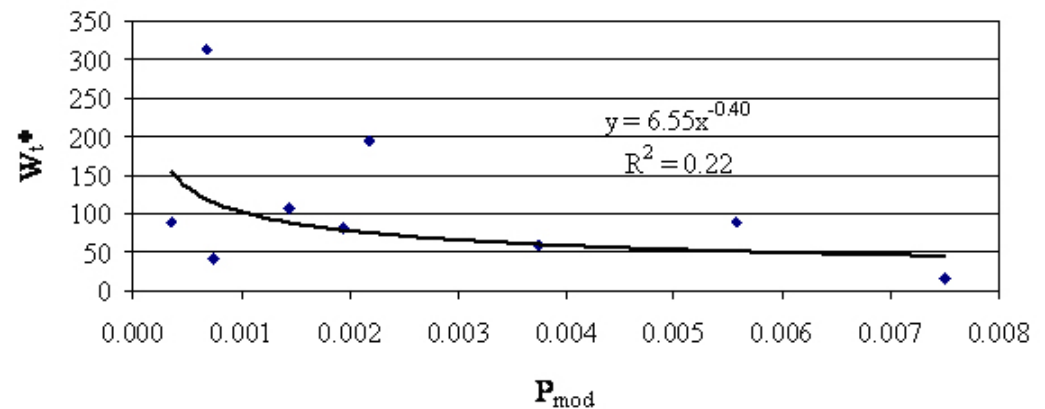


$$P = \frac{h_p - h_0}{t_d u_{*0}}$$

$$P_{\text{mod}} = \frac{h_p - h_0}{t_r \left( \frac{u_o + u_p}{2} \right)} \frac{u_{*p}^2 - u_{*cr}^2}{u_{*cr}^2}$$

$$\frac{W_t}{\rho_s B D_{50}^2}$$

nondimensionalized total bed load





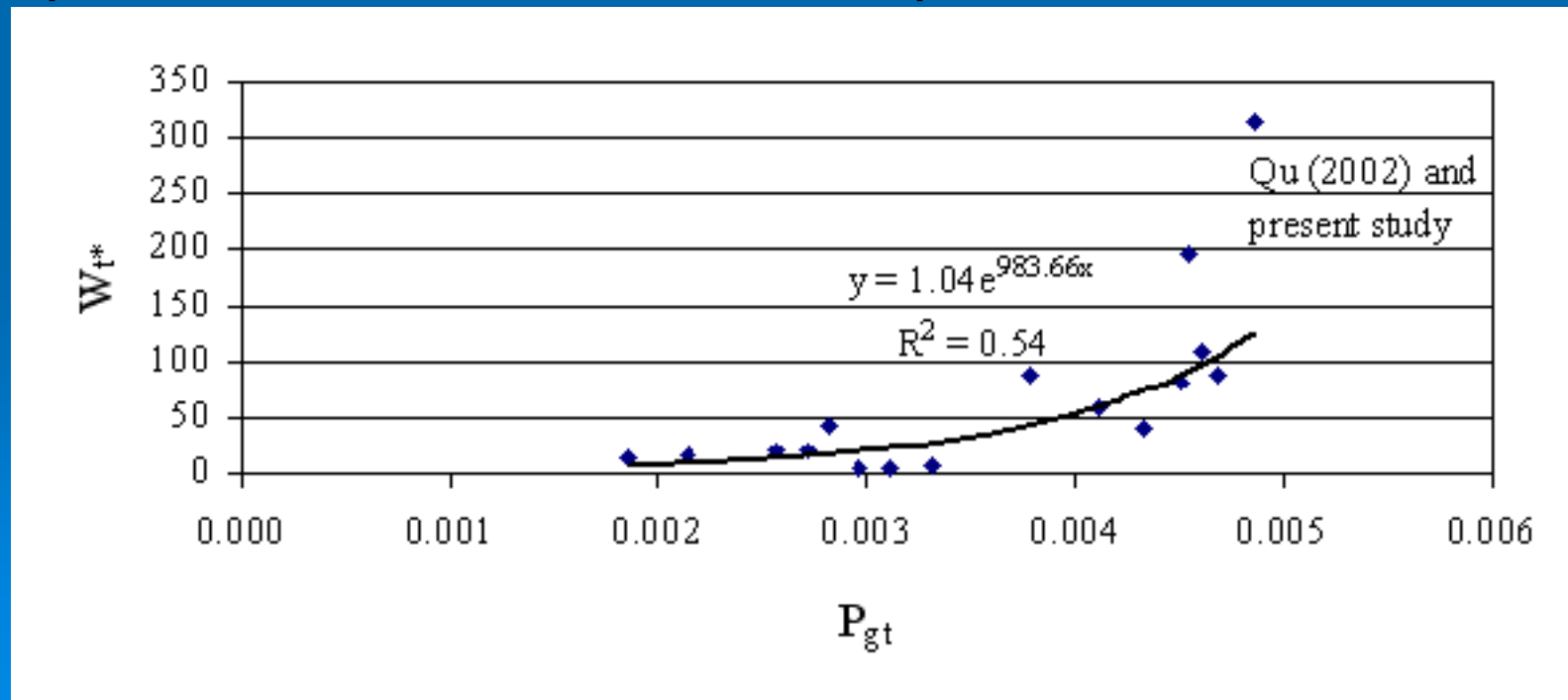
## Case Study: Unsteadiness Parameter and Total Flow Work

- Unsteady regime causes resuspension and transport of deposited bottom sediments. This is because turbulence intensities, both streamwise and vertical, are larger in unsteady flows, causing lift forces onto sediment particles. According to Graf (2003) turbulence plays an essential role in all flows of water-sediment mixture.
- This has forced us to come to a conclusion  $P$  and  $P_{mod}$  may not be proper expressions to express the unsteadiness effects of a flow either for short duration hydrographs or for the experiments carried out in this study. Therefore, in this study, we proposed the following formulation based on the concept of net acceleration for expressing unsteadiness parameter.

$$P_{gt} = \frac{\left| gS_o - \left( \frac{u_p - u_o}{t_r} \right) \right|}{g}$$

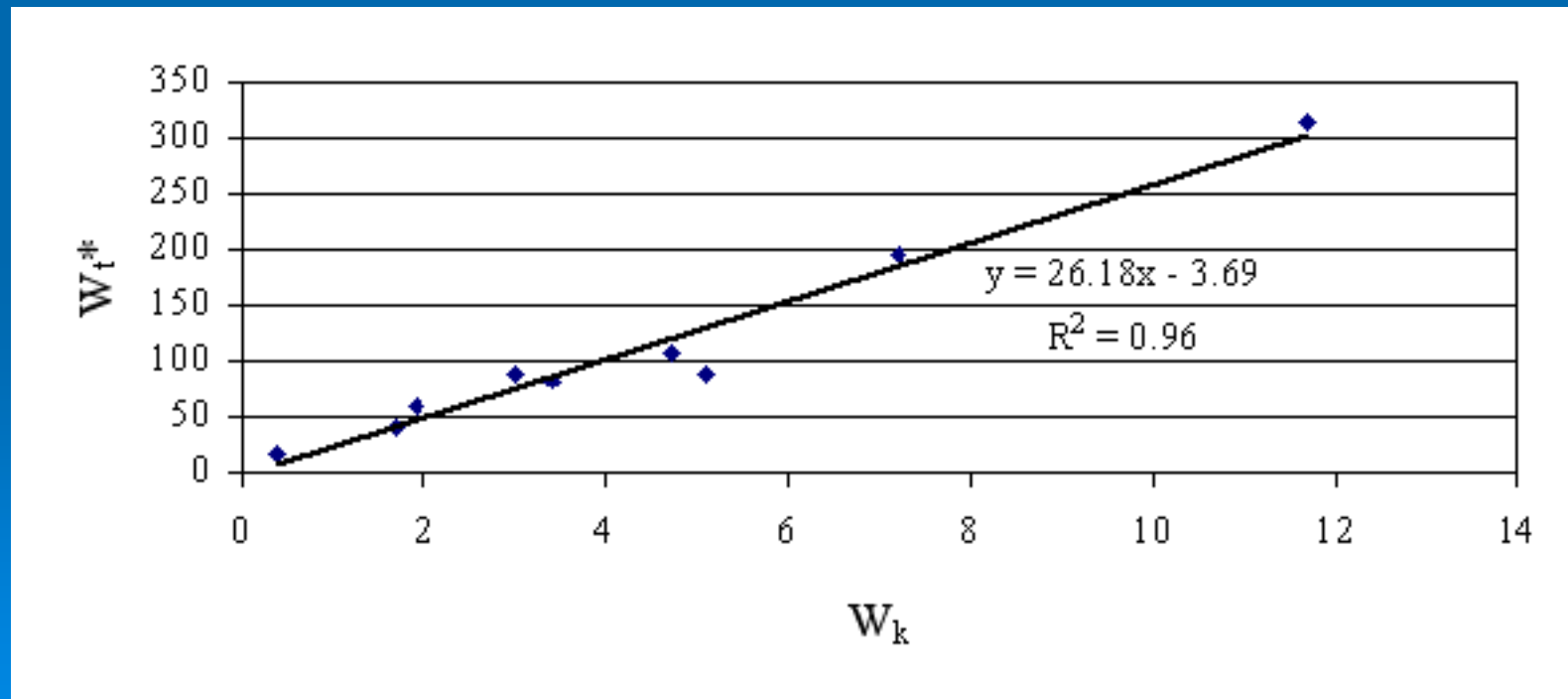
## Case Study: Unsteadiness Parameter and Total Flow Work

- For the verification of the proposed parameter,  $P_{gt}$ , the parameter was tested with an independent set of data with different bed slope. The bed slope used in the experiments conducted by Qu (2002) was 0.003, whereas in our experiments we utilized a bed slope of 0.005.



## Case Study: Unsteadiness Parameter and Total Flow Work

- The variation between the dimensionless total bed load and total flow work. As seen, there is a strong linear variation between the two variables with  $R^2 = 0.96$ .



# Case Study: Simulation of Experimental Results

- One dimensional unsteady bedload transport equations which are based on the conservation of mass for water and sediment and the dynamic momentum equation approximated by the diffusion wave are utilized (Singh and Tayfur 2008):

$$\frac{\partial h}{\partial t} + \frac{\partial hu}{\partial x} + p \frac{\partial z}{\partial t} = 0$$

$$\frac{\partial h}{\partial x} + \frac{\partial z}{\partial x} = S_o - S_f$$

$$(1-p) \frac{\partial z}{\partial t} + \frac{\partial q_{bs}}{\partial x} = 0$$

- The system can be closed by employing, respectively, the Chezy's formulation for friction slope and the kinematic wave theory for the sediment flux (Tayfur and Singh 2006) as:

$$u = C_z \sqrt{RS_f}$$

$$q_{bs} = (1-p)v_s z \left[ 1 - \frac{z}{z_{\max}} \right]$$

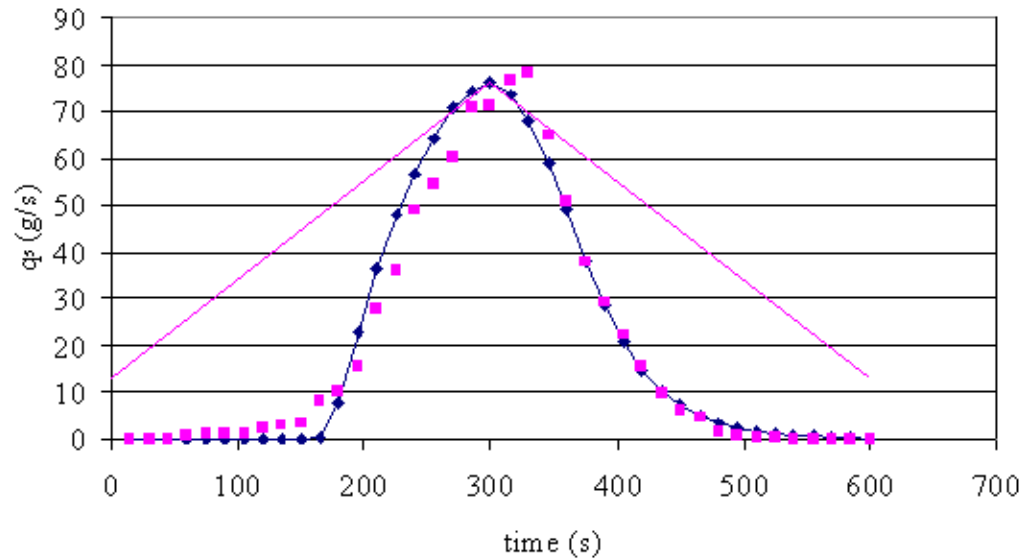
$$C_z = \frac{R^{1/6}}{n}$$

- For particle velocity, the approach proposed by Chien and Wan (1999) can be employed:

$$v_s = u - \frac{(u_c / 1.4)^3}{u^2}$$

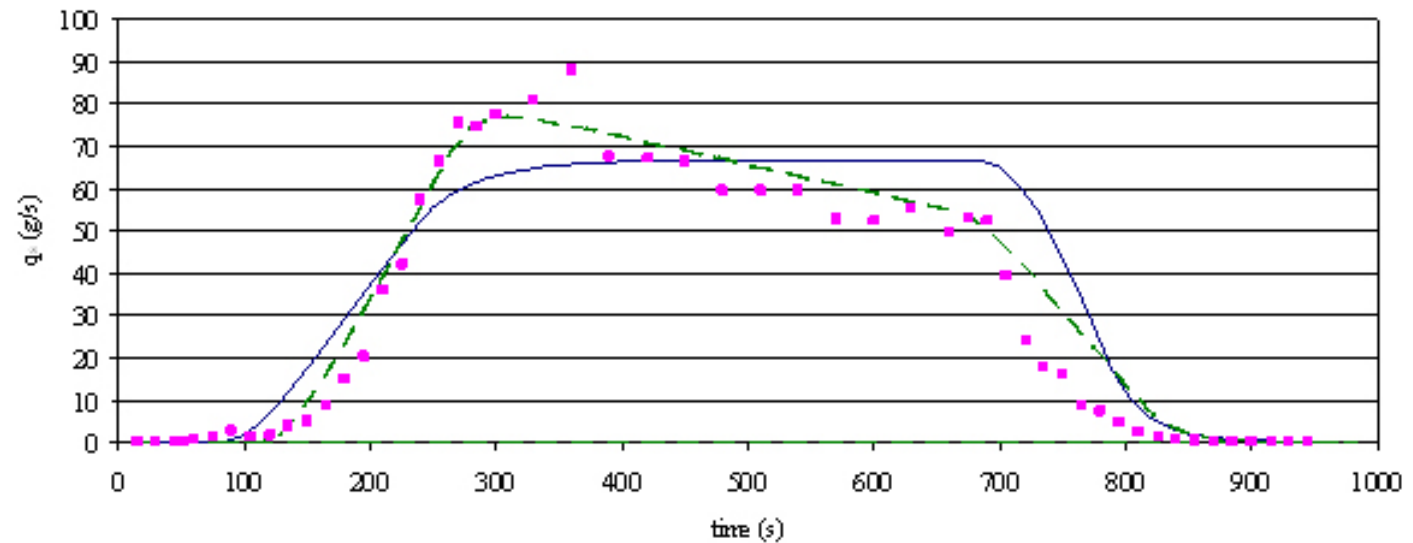
## Case Study: Simulation of Experimental Results

- The system of equations is solved using the Lax finite difference method.
- Parameters used in the numerical model are consistent with the experiments where a channel with a length of 18 m, a width of 0.80 m and slope of 0.005 is modeled, porosity is taken as 0.4 and sediment density and size are set to  $2640 \text{ kg/m}^3$  and 4.8 mm respectively.
- The initial water depth is set to baseflow depth and initial elevation of the bed is set to 8 cm. At the upstream boundaries water depth and bed elevation are set to values calculated for the corresponding time step and a Neumann boundary condition (zero gradient) is applied for the downstream boundaries. In the simulations, the space step is taken as 0.10 m.



—◆— modeled sediment yield    ■— observed sediment yield    — discharge

Comparison of the numerically modeled sediment yield with the observed sediment yield



— modeled data with uniform sand    ■— observed data    - - modeled data with non-uniform sand

- The model satisfactorily simulated the rising and recession limbs of the sedimentographs, underpredicted the equilibrium portion when strictly uniform small gravel, i.e., a constant value of  $D_{50} = 4.8$  mm was considered.
- The numerical model was modified to transport mixture of sediments. The governing equations for the transport of mixture sediment as a bed load (Armanini and di Silvio 1988; Wu et al 2004):

$$\frac{\partial h}{\partial t} + \frac{\partial hu}{\partial x} + \sum_{i=1}^N p_i \left( \frac{\partial z}{\partial t} \right) = 0$$

$$\frac{\partial h}{\partial x} + \sum_{i=1}^N \left( \frac{\partial z}{\partial x} \right) = S_o - S_f$$

$$\left( 1 - \sum_{k=1}^N p_i \right) \frac{\partial z}{\partial t} + \sum_{i=1}^N \left( \frac{\partial q_{bs}}{\partial x} \right) = 0$$

